NASA Technical Paper 1121

Effects of Fabrication and Joining Processes on Compressive Strength of Boron/Aluminum and Borsic/Aluminum Structural Panels

Dick M. Royster, H. Ross Wiant,
and Robert R. McWithey

APRIL 1978

NASA

NASA Technical Paper 1121

Effects of Fabrication and Joining Processes on Compressive Strength of Boron/Aluminum and Borsic/Aluminum Structural Panels

Dick M. Royster
Langley Research Center, Hampton, Virginia
H. Ross Wiant
Vought Corporation, Hampton, Virginia
Robert R. McWithey
Langley Research Center, Hampton, Virginia

National Aeronautics
and Space Administration

**Scientific and Technical
Information Office**

1978

SUMMARY

Methods for forming and joining boron/aluminum and Borsic/aluminum to themselves and to titanium alloys have been studied at the NASA Langley Research Center. The present study was conducted to determine the effects of joining and fabrication methods on panel compressive strengths for composite skin and titanium skin panels with composite stringers. The stringers and panel skins were joined by high strength bolts, by spotwelding, by diffusion bonding, by adhesive bonding, or by brazing. The test results show that hot and cold forming of metal-matrix composite stringers did not degrade fiber properties, whereas a eutectic consolidation and fabrication process did cause fiber degradation. Of the processes investigated for joining the metal-matrix stringers, the diffusion-bonded and adhesive-bonded panels developed the highest buckling loads and stresses. A program for predicting buckling loads (BUCLASP2) consistently predicted higher buckling loads than were determined experimentally.

INTRODUCTION

The National Aeronautics and Space Administration (NASA) is investigating advanced resin-matrix and metal-matrix composite materials to determine whether their low mass and favorable mechanical properties can be used in aerospace vehicles. A key area of this research is manufacturing technology. Methods for joining boron/aluminum and Borsic/aluminum composites to themselves and to titanium alloys are being studied at the NASA Langley Research Center (ref. 1).

The purpose of this study was to determine the effects of joining and fabrication methods on compressive strengths of two skin-stringer configurations. One configuration consisted of composite skin panels stiffened with composite stringers, and the second configuration consisted of titanium skin panels stiffened with composite stringers. Hat-shaped stringers were joined to the skin panels by high strength bolts, by spotwelding, by diffusion bonding, by adhesive bonding, or by brazing. The test data include maximum load, buckling load, and fiber strength for these skin-stringer panels. Predicted buckling loads are compared with the experimental data. Results of metallurgical examinations of the skin-stringer bonds for the different joining methods are presented also.

The physical quantities defined in this paper are given both in the International System of Units (SI) and in the U.S. Customary Units. Measurements and calculations were made in the U.S. Customary Units. Factors relating the two systems are given in reference 2 and those used in this investigation are presented in appendix A.

PROCEDURES

Materials

Photographs of typical hat-shaped stringers and skin-stringer panels are shown in figures 1 and 2, respectively. Material used in the fabrication of hat-shaped stringers was either boron/aluminum (B/Al) or Borsic/aluminum (Bsc/Al), while the skin material was B/Al, Bsc/Al, or Ti-6Al-4V titanium alloy. The nominal fiber volume for each composite material was 48 percent. All skins and stringers were obtained from commercial sources.

Skins.- The metal-matrix skin material consisted of 9 plies of either 0.1422-mm (0.0056 in.) diameter boron fiber or 0.1448-mm (0.0057 in.) diameter Borsic fiber aligned unidirectionally in a 6061 aluminum alloy matrix. The nominal skin thickness was 1.676 mm (0.066 in.). All the B/Al and Bsc/Al skin materials were fabricated and supplied by one source. The Ti-6Al-4V titanium alloy skin material was 1.346 mm (0.053 in.) thick and was supplied in the annealed condition.

Stringers.- The metal-matrix stringer material consisted of 7 plies of boron fiber or Borsic fiber aligned unidirectionally in a 6061 aluminum alloy matrix. Hat-shaped stringers, of the configuration shown in figure 1, were fabricated from these materials by using a hot forming process, a cold forming process, or a eutectic bonding process.

In the hot forming process, a stainless steel caul sheet, 0.635 mm (0.025 in.) thick, was positioned on the side of the composite sheet that was in tension during forming. This method helped prevent cracks from occurring in the bend of the composite material. Production of one hat-shaped stringer required four separate forming operations, one for each bend, with the caul sheet shifted to the tension side for each bend. Each bend was formed in a heated die after the caul sheet and composite material were exposed for 5 minutes to the forming temperature of 728 K (850° F). After forming each bend, the die remained in the closed position for 1 minute. Final sizing of the stringer was performed in a hot sizing fixture to ensure that the stringer elements would be straight.

For the cold forming process, B/Al composite sheet was supplied with 0.635-mm (0.025 in.) thick mild carbon steel diffusion bonded to the exterior surfaces to improve the ambient-temperature formability of the composite sheet. The steel was selectively etched from the composite sheet surface in the area of the bend that would be placed in compression during forming. The sheet was immersed in a 50-percent nitric acid solution which removed the steel without affecting the composite sheet. The composite sheet was placed in the die and the bend was formed with the steel on the tension side of the bend forcing the neutral axis to shift toward the steel cladding. This process lowered the tensile stresses in the composite sheet and reduced the chance of cracks occurring in the bend. After the bend was formed, the remaining steel was completely removed from the stringer by nitric acid etching. Final sizing was identical to that performed on the hot-formed stringers.

In the eutectic bonding process, the stringers were fabricated by stacking seven plies of monolayer B/Al material with 0.46 μm (18×10^{-6} in.) of copper vapor deposited on each surface, hot isostatic pressing to the required stringer shape, and consolidating by eutectic bonding. The time-temperature-pressure relationship for the eutectic bonding process consisted of approximately 10 minutes at a temperature between 828 and 844 K (1030° and 1060° F) in an autoclave at a pressure of 2.03 MPa (295 psi).

Test Specimens

The skin-stringer panel, used to characterize the different joining methods for the composite materials, is shown in figure 2. The skins and hat-shaped stringers were joined by high strength bolts, by resistance spotwelding, by diffusion bonding, by adhesive bonding, or by brazing. The filament orientation in the skins and stringers was always in the longitudinal direction of the stringers. Figure 3 shows the cross section and table I gives the dimensions and mass of each panel investigated.

To determine the effects of fabrication and joining processes on panel compressive strength, both panel geometry and boundary conditions were kept constant, within state-of-the-art capabilities, for panels having a given skin material. Fabrication processes were expected to affect panel strength because of degradation of matrix strength and modulus, variations in fiber volume fraction, and deviations from the nominal panel geometry. Joining procedures were expected to affect panel strengths because elevated-temperature joining processes can cause material degradation. Also variations in the geometry of the joints affect the local flexibility of the stringers relative to the skins, with possible effects on the local buckling strengths of the panels. Therefore, the panels were designed to exhibit local crippling failure by choosing panel dimensions and boundary conditions that prevented Euler buckling but allowed simultaneous local buckling of the flat-plate elements within the panel cross section at a strain below the yield strain of the panel materials. In keeping with this criterion, the unsupported width b and thickness t of each element were selected to have a nominal flat-plate b/t ratio of 30 for the composite skin-stringer elements and 38 for the titanium skin-stringer elements. Each of these b/t ratios results in a predicted buckling strain of approximately 0.0026. All the stringers met this criterion except for the eutectically bonded stringers which had b/t ratios of 33 for the panels with composite skins and 42 for the panels with titanium skins. The variance in b/t ratios precluded making comparisons of the loads developed in panels having eutectically bonded stringers with the loads developed in panels having either hot- or cold-formed stringers.

Joining Methods

The B/Al and the Bsc/Al stringers were supplied 260.4 mm (10.25 in.) long so that no machining or sizing was required prior to joining to the skins. The composite skin material was supplied in 3048-mm by 178-mm (120 in. by 7 in.) sheets and was cut to 260.4 mm by 152.4 mm (10.25 in. by 6.0 in.) with a conventional diamond-wheel saw. Prior to joining the skins and stringers, both

were given a surface preparation as outlined in appendix B. After surface preparation, the panel parts were assembled by the methods given in the following sections.

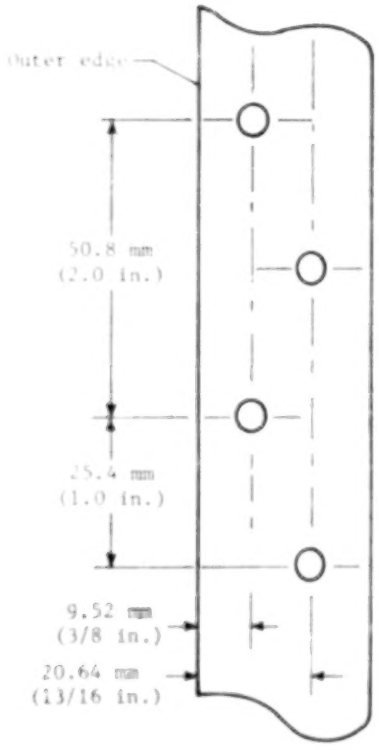

High strength bolts.- The titanium and B/Al skins were attached to B/Al stringers with 4.76-mm (3/16 in.), hexagonal-head steel bolts and nuts. Holes were drilled in the B/Al skins and stringers with a diamond core drill. The holes in the titanium alloy skins were drilled with high speed steel drills. The holes through each stringer flange were drilled in two rows (as shown in sketch at left), with the center lines located 9.52 mm (3/8 in.) and 20.64 mm (13/16 in.) from outside edge of the flange. The holes in each row had a 50.8-mm (2.0 in.) pitch, with the centers of the holes in one row staggered 25.4 mm (1.0 in.) from the centers of the holes in the other row. The bolted assembly had 12.7-mm (1/2 in.) outside-diameter washers on both outer surfaces. Final assembly torque was 2.8 N·m (25 lbf·in.). After assembly, the panels were wiped clean with acetone.

Resistance spotwelding.- A standard 100-kVA spotwelder was used to attach panel skins to hat-shaped stringers with a single row of resistance spotwelds along each flange. The spotwelds had a pitch of 19.05 mm (0.75 in.) in each row, and the rows were 68.58 mm (2.70 in.) apart, measured at the center lines. The size of the weld nugget and the failure loads measured in single-lap shear quality control tests are given in the following table:

Material	Nugget diameter, mm (in.)	Failure load, kN/spotweld (lbf/spotweld)
B/Al to B/Al	7.62 (0.30)	6.89 (1550)
B/Al to Ti	7.62 (0.30)	6.83 (1535)
Bsc/Al to Bsc/Al	7.87 (0.31)	8.50 (1910)
Bsc/Al to Ti	7.87 (0.31)	7.45 (1675)

Diffusion bonding.- Skin panels were attached to hat-shaped stringers by a continuous diffusion bond along each flange. Bonding pressures and temperatures were attained in a 890-kN (100 ton) capacity laboratory press equipped with heated platens. Bonding was accomplished in a retort which permitted controlled heating and loading under a vacuum of approximately 3.33 Pa (0.025 torr). To promote diffusion bonding at acceptably low temperatures and

pressures, 0.051-mm (0.002 in.) 2024 aluminum alloy foil was used between mating surfaces. Diffusion bonding parameters were 811 K (1000° F) for 15 minutes at 10.3 MPa (1500 psi) pressure. Distortions of the skin-stringer assembly were limited by the use of a mild-steel, form-fitting filler bar inserted within the hat-shaped stringer.

Adhesive bonding.- The adhesive tape system, designated LARC-3, used to bond the skin-stringer panels was developed at the Langley Research Center. (See ref. 3.) The stringers and skins were assembled in a bonding fixture with adhesive covering the flange attachment area. The bonding fixture was then placed in a heated platen press, and the bonds were cured at 611 K (640° F) and 1.38 MPa (200 psi) for 1 hour.

Brazing.- Bsc/Al stringers were brazed to Bsc/Al skins and to Ti-6Al-4V titanium alloy skins with either 0.076-mm (0.003 in.) thick 4047 aluminum brazing foil (AWS-ASTM BAlSi-4)[1] or 0.127-mm (0.005 in.) thick "braze sheet," a commercial brazing sheet composed of 0.102-mm (0.004 in.) 3003 aluminum alloy clad on both sides with 0.0127-mm (0.0005 in.) thick 4047 aluminum alloy. The basic joining fixture utilized titanium honeycomb tooling. Pressure was applied to the brazed joint by a stainless steel inflatable diaphragm located on top of the brazing pack. The stringer and skin were assembled with the selected brazing foil positioned between the mating surfaces. Alignment was maintained by small, resistance tack welds at the extreme ends of the stringer flanges. Panels were brazed in a vacuum furnace at 861 K (1090° F) for 5 minutes. Pressure in the joint was maintained at 34.5 kPa (5 psi) by use of the inflatable diaphragm.

Tests

After the panels were fabricated, the ends of each panel were "potted" with a room-temperature-cure epoxy compound. This treatment facilitated machining the panel ends to test length. (See table I.) Potting also prevented crushing or "brooming" of the panel ends during the tests. The skins were clamped against a flat plate, and the ends of the panels were machined flat and parallel to each other and perpendicular to the longitudinal axis of the panels. To ensure uniform loading through the panel, the ends of each panel were checked, after machining, for parallelism and flatness by placing the panel between parallel heads of a test machine, applying a small load, and inserting a feeler gage between each head and the machined end of the panel. The distance between the machined panel end and the test machine head was less than 0.051 mm (0.002 in.) for all the panels, and they were thus found to be acceptable for testing. Before the axial compression tests, each panel was instrumented with strain gages on the skin and stringer as shown in figure 4. Linear variable differential transformers (LVDT) were used to measure panel shortening. The test setup for the panels is shown in figure 5. The edges of the panels were simply supported with knife edges positioned 6.35 mm (0.25 in.)

---

[1]Available commercially as Alcoa No. 718 brazing sheet from Aluminum Company of America.

from each panel edge. Outputs from strain gages, LVDT's, and the load indicator were recorded during the tests.

A preload of 4.4 kN (1 kip) was applied to check the recording system. The panels were then loaded to failure at a rate of approximately 44.5 kN/min (10 kips/min). Data were recorded every 10 seconds until local instability was detected and every second thereafter until maximum load was reached.

Metallurgical Investigation

After the compression tests of the skin-stringer panels, samples were cut from undeformed regions for metallographic examination of representative cross sections of the composite materials and of the panel joints. The samples were mounted in phenolic resin, polished, and examined on a metallograph. All photomicrography was performed under a bright field using a green interference filter. The photomicrographs were studied to determine the quality of the joints and to identify metallurgical changes, in either the composite or the titanium, due to fabrication.

RESULTS AND DISCUSSION

The skin-stringer panels joined by high strength bolts, by spotwelding, by adhesive bonding, by diffusion bonding, or by brazing were tested in axial compression. The data obtained from the tests are presented in figures 6 to 8 and tabulated in table II. The two LVDT load-shortening curves shown in figure 6 are for diffusion-bonded panels with a B/Al skin (fig. 6(a)) and with a titanium skin (fig. 6(b)). These curves are typical of all the load-shortening curves obtained from the LVDT's in that, for a given skin material, the initial slopes are similar and the curves are generally linear up to the onset of local elastic buckling in the skins. The average strain detected by the four strain gages prior to local elastic buckling, as indicated by strain reversal, is also plotted on the curves as $\bar{\epsilon}$ (and tabulated in table II for all the panels) at the load where strain reversal occurred. At the maximum load, failure occurred by instantaneous crippling of the stringer and skin.

Panel Maximum Stress

The average maximum stress in each panel is shown in figure 7. The average maximum stress is defined as the maximum compressive load sustained by the panel divided by the cross-sectional area of the panel as given in table I. In the figure, the panels are grouped according to the skin material and joining process with the letters H, C, and E denoting hot-formed, cold-formed, and eutectically bonded stringers, respectively.

Two evaluations are of interest, that is, the effects of stringer fabrication and of joining processes on the maximum stresses. Generally, for the same joining process and skin material, a higher average maximum stress was obtained from panels with cold-formed stringers than from panels with hot-formed stringers. For the same stringer fabrication method and skin material, the diffusion

bonding process generally gave the highest average maximum stress. The adhesive bonding or brazing processes generally exhibited higher average maximum stresses than the spotwelding or bolting processes. Thus, the panels with continuously bonded skin-stringer joints exhibited higher average maximum stresses than the panels with discontinuously bonded skin-stringer joints.

Panel Buckling Load

The buckling loads of all the panels are shown in figure 8 and tabulated in table II. In the figure, the panels are grouped according to skin material and joining process. The experimental buckling loads of the panels were determined from strain gage data. The lowest load at which strain reversal occurs, as determined from any one of four strain gages mounted on the panels, is recorded as the buckling load. The highest buckling loads were exhibited by the diffusion-bonded and adhesive-bonded panels with B/Al skins and either cold-formed or hot-formed B/Al stringers.

The dashed lines in the figure are the buckling loads predicted for the panels by the BUCLASP2 program (ref. 4). This program is designed to perform linear elastic buckling analysis on structures with constant cross sections that may be idealized by an assembly of flat- and curved-plate elements and beam elements.

The program inputs are described in appendix C and an analysis of the data derived from the BUCLASP2 program is presented. Briefly, the program was modeled to account for panels with continuous joints (adhesive bonding, diffusion bonding, and brazing) and for panels with discontinuous joints (spotwelding). Since the BUCLASP2 program could not model the staggered attachment of the bolted panels, no predictions were made for these panels. The graphical comparisons between analytical and experimental buckling loads (shown in fig. 8) indicate that the analytical buckling loads are always higher than the experimental values. Analytical values range from approximately 1 percent higher than the experimental values for the diffusion-bonded panels, with B/Al skins and hot- or cold-formed stringers, to 56 percent higher than the experimental values for the spotwelded panels, with B/Al skins and eutectically bonded stringers.

Panel Failures

Typical failures of the panels in axial compression are shown in figure 9. The integrity of the joints was maintained until panel failure. All panels exhibited local buckling prior to instantaneous crippling of the stringer and skin. The bolted panels exhibited longitudinal fractures in the stringer, adjacent to the innermost row of bolt holes (fig. 9(a)). Typical for some of the panels (diffusion bond and adhesive bond) is the longitudinal fracture of the composite stringer in the radius of the attachment flanges (figs. 9(b), (c), (d), and (e)). In addition, most of the diffusion-bonded and adhesive-bonded panels exhibited transverse fractures of the composite material in the stringer across the center of the panels (figs. 9(b), (c), (d), and (e)), and longitudinal fractures in the composite skins adjacent to the attached flanges

of the stringer (figs. 9(c), (d), and (e)). Considerably more deformation and tearing occurred in these panels than in panels joined by other processes. The Bsc/Al panels (figs. 9(f) and (g)) did not exhibit composite fractures in either the spotwelded or brazed panels. A few spotwelds failed in the center of most panels where maximum deformations occurred. Some separation of stringer and skin occurred in the adhesive-bonded panels at maximum loads. Examination of the failed panels revealed that the panels that developed the highest strength (i.e., diffusion-bonded and adhesive-bonded panels) exhibited more composite fracture and deformation than did the panels that developed lower strength (i.e., bolted, spotwelded, and brazed panels).

Fiber Strength

In order to determine the effects of thermal processing on the strength of the boron and Borsic fibers, samples were cut from the stringer and skin of the tested panels. The fibers were removed from the samples by leaching away the aluminum matrix in a sodium hydroxide solution. The strengths of the fibers were qualitatively determined by bend tests. (See test fixture described in ref. 1.) The effects of fabrication and joining on fiber strength are shown in figure 10 where the average fiber strengths are shown for each joining procedure. Each bar represents the average of approximately 40 fiber tests. The spotwelded and bolted panels, by nature of their joining processes, did not receive any thermal treatment other than the temperatures associated with material consolidation and stringer fabrication. Therefore, the strength of the fibers from these panels was used as a reference to compare with the strengths of fibers from the remaining panels and to determine the effect of the joining process on fiber strength. For example, the boron fibers from the skins of diffusion-bonded panels show a loss in strength of approximately 4 percent (fig. 10(a)). Although this reduction in fiber strength is small, the degradation may be due to the temperature involved in the diffusion bonding process. The strength of boron fibers from the skins of adhesive-bonded panels appears to be unaffected by the temperature associated with the adhesive bonding process.

The strength of boron fibers from the stringers is shown in the lower portion of figure 10(a). As expected, the strength of fibers from the hot- and cold-formed stringers was generally the same as was found in fibers removed from the skin material. However, fibers obtained from stringers fabricated by the eutectic consolidation process had low strength. For these fibers, the average strength was 2.34 GPa (340 ksi), or 25 percent less than the strength of fibers from the hot- or cold-formed stringers. A certificate of conformance supplied with the stringers showed that prior to consolidation by the eutectic consolidation process the fibers had high strength. Evidently the temperatures (828 to 844 K (1030° to 1060° F)) used in the eutectic bonding process caused degradation of the fibers. The lower strength of fibers in the eutectically consolidated stringers may explain the lower loads and stresses developed during the compression tests by panels with these stringers.

The results of strength tests on Borsic fibers are shown in figure 10(b). The strength of fibers from brazed panels is approximately 10 percent lower

than the strength of fibers from spotwelded panels and indicates fiber degradation due to the brazing process.

Metallurgical Investigation

Matrix.- The photomicrographs in figure 11 are typical of the composite microstructure in the "as received" condition. Figure 11(a) represents a typical microstructure for the B/Al or Bsc/Al skin material after the consolidation process. The appearance of a second bond line snaking between the fiber layers is evidence that double sheets of the 6061 aluminum foil had been used in the consolidation. The photomicrographs of figures 11(b) and (c) show typical microstructures of B/Al stringers after cold forming and hot forming, respectively. The microstructure of these stringers is similar to the microstructure of the skin (fig. 11(a)). The microstructure in figure 11(d) illustrates a section of stringer fabricated by the low pressure, eutectic bonding process. With this process, boron/6061 aluminum monolayer tape is consolidated into a multilayer sheet by using vapor deposited copper to promote diffusion. Note the nearly straight monolayer interfaces which indicate previously consolidated monolayer sheet surfaces. The copper deposited on the 6061 aluminum diffused into the matrix and caused broadening of the grain boundaries through copper enrichment (see fig. 11(d)) which could result in a significant lowering of the transverse tensile properties in the unidirectional composite material.

Spotwelds.- Cross sections of resistance spotwelds are shown in the photomicrographs of figure 12. Disruption of the normal fiber distribution is common to all of the weld cross sections observed. The cross section of a spotweld joining B/Al to B/Al (fig. 12(a)) shows a "nugget" or molten zone common to both parts of the joint. The titanium-B/Al resistance spotweld (fig. 12(b)) is in reality a diffusion bond. In the short time and high pressure normally associated with resistance welding, only the aluminum matrix in the composite melted and bonded to the titanium. The appearance of a "nugget" in the titanium is only a heat-affected zone with no evidence that the titanium melted.

Adhesive bond.- The LARC-3 adhesive bond between a B/Al skin and a B/Al stringer is shown at two magnifications in figure 13. Note that the thickness of the adhesive (fig. 13(a)) is approximately equivalent to one ply of B/Al. Also note one of the numerous places where fibers in the composite material were exposed by the etchant used to prepare the surface for bonding. The higher magnification photomicrograph (fig. 13(b)) shows the details of the glass-fiber carrier and aluminum filler in the adhesive.

Diffusion bond.- Cross sections of diffusion bonds are shown in the photomicrographs of figure 14. At the time-temperature-pressure parameters required to form the diffusion bond, a very small quantity of liquid phase was present in the 2024 aluminum foil used to promote diffusion between the composite stringer and the composite or titanium skin. Note that the bonds appear to be of excellent quality with little or no effect on the matrix microstructure beyond the middle of the first ply of boron.

Brazing.- The joint shown in figure 15 was produced by positioning 0.076 mm (0.003 in.) of BAlSi-4 brazing foil between a B/Al stringer and a

titanium skin and brazing at 861 K (1090° F). A result of the brazing is the increased number of silicon particles in the braze area and in the immediately adjacent matrix. Since some minor incipient melting of the 6061 aluminum alloy matrix occurs at temperatures between 855 and 866 K (1080° and 1100° F), some liquid-liquid diffusion occurred. Silicon diffusion at these temperatures was reported to be exceedingly rapid (ref. 1). The extent of this diffusion is readily evident by the high content of silicon in acicular form between the first and second plies of Borsic fibers. Examinations of the sample shown in figure 15 were made with a scanning electron microscope (SEM) to determine the extent of silicon diffusion into the 6061 aluminum matrix. Significant areas of silicon were detected in the grain boundaries from the braze interface to the fourth ply of Borsic fibers.

The photomicrographs in figure 16 show Bsc/Al stringers brazed to Bsc/Al and titanium skins with braze sheet used to minimize the quantity of 4047 aluminum available for matrix interaction. The brazing technique used with the braze sheet was identical to that used with BAlSi-4 brazing foil. The 6061 aluminum matrix shows distinct evidence of interdiffusion with the 4047 aluminum cladding on the braze sheet in both figures 16(a) and (b). However, the use of braze sheet minimized the diffusion of the brazing alloy into the matrix with no indication of silicon past the first ply of Bsc/Al.

The overall effect of silicon diffusing into the 6061 aluminum matrix is to embrittle the matrix and reduce its strength. This effect, combined with the Borsic fiber degradation discussed previously, apparently caused the strength of the brazed Bsc/Al skin-stringer panels to be lower than the strengths of the other continuously bonded panels. (See figs. 7(c) and (d).)

Other brazing studies on Bsc/Al (refs. 1 and 5) have shown that successful brazed joints can be made with a minimum of fiber/matrix degradation. This is accomplished by using 0.127 mm (0.005 in.) of 1100 aluminum alloy as an outer layer to serve as a diffusion barrier between the braze and matrix.

CONCLUDING REMARKS

An investigation was conducted to determine the effects of fabrication and joining methods on the compressive strengths of panels with boron/aluminum, Borsic/aluminum, or titanium skins and with boron/aluminum or Borsic/aluminum hat-shaped stringers. The joining methods included high strength bolts, spot-welding, diffusion bonding, adhesive bonding, and brazing. The following results were found:

1. Boron/aluminum or Borsic/aluminum stringers fabricated from consolidated flat sheets by hot or cold forming processes had fiber properties essentially equal to original values.

2. A eutectic consolidation process for fabricating boron/aluminum stringers caused degradation in fiber strength of at least 25 percent.

3. Compression tests of the panels and metallurgical investigation of the joints indicate that the integrity of the joints was maintained until panel failure.

4. Of the joining processes investigated, diffusion bonding and adhesive bonding produced skin-stringer panels which developed the highest compressive stresses.

5. The low stresses developed by the brazed Borsic/aluminum skin-stringer panels were apparently caused by reduced matrix and fiber strengths which resulted from braze-matrix interaction.

6. Panels made with discontinuous joining methods (bolted and spotwelded) exhibited joint failures, whereas panels made with continuous joining methods (diffusion bonded and adhesive bonded) exhibited failures in the radius of the attachment flange and across the crown of the stringer.

7. Analytical buckling loads predicted by the BUCLASP2 program were higher than the experimentally determined buckling loads.

Langley Research Center
National Aeronautics and Space Administration
Hampton, VA 23665
February 28, 1978

APPENDIX A

CONVERSION OF U.S. CUSTOMARY UNITS TO SI UNITS

Conversion factors (from ref. 2) required for units used herein are given in the following table:

Physical quantity	U.S. Customary Unit	Conversion factor (a)	SI Unit (b)
Force	kip = 1000 lbf	4.448×10^{3}	newton (N)
Length	in.	2.54×10^{-2}	meter (m)
Mass	lbm	4.536×10^{-1}	kilogram (kg)
Mass/volume	ounce/gallon	7.489	kilogram/meter^3 (kg/m^3)
Stress	kip/in^2 (ksi) psi	6.895×10^{6} 6.895×10^{3}	pascal (Pa) pascal (Pa)
Pressure	torr	1.333×10^{2}	pascal (Pa)
Temperature	^{o}F	(^{o}F + 459.67)/1.8	kelvin (K)
Torque	pound force-inch	1.130×10^{-1}	newton meter (N·m)

[a]Multiply value given in U.S. Customary Unit by conversion factor to obtain equivalent value in SI Unit.

[b]Prefixes to indicate multiples of SI Units are as follows:

Prefix	Multiple	Symbol
micro	10^{-6}	μ
milli	10^{-3}	m
kilo	10^{3}	k
mega	10^{6}	M
giga	10^{9}	G

APPENDIX B

SURFACE PREPARATION PROCESSES

Spotwelding, Diffusion Bonding, and Brazing

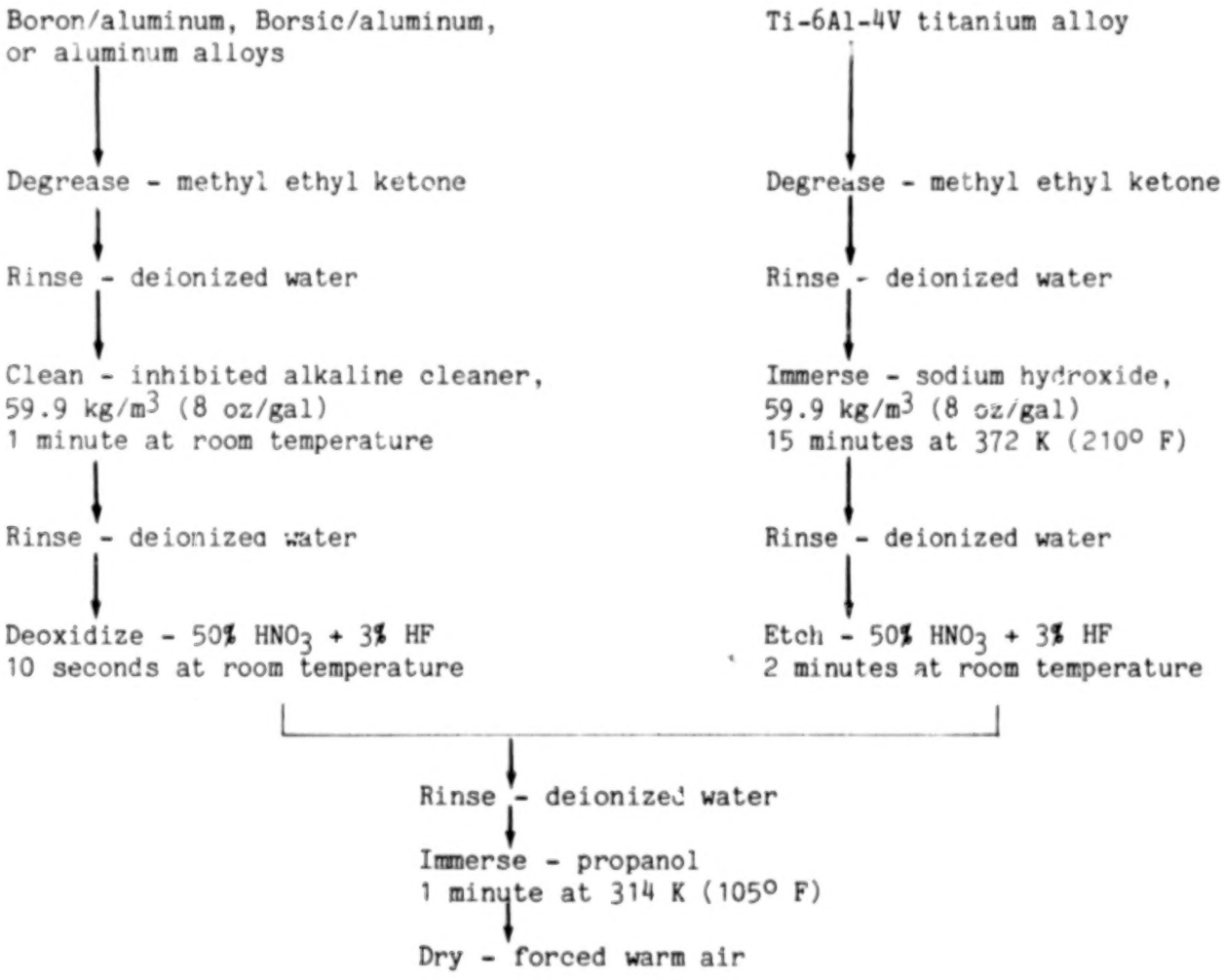

APPENDIX B

Adhesive Bonding

Boron/aluminum

↓

Degrease - trichloroethylene
5 minutes

↓

Immerse in solution of:
sodium hydroxide, 37.4 kg/m^3 (5 oz/gal)
sodium carbonate, 15.0 kg/m^3 (2 oz/gal)
sodium phosphate, 22.5 kg/m^3 (3 oz/gal)
30 seconds at 344 K (160° F)

↓

Rinse - tap water
1 minute

↓

Etch - distilled water, 30 parts
sulfuric acid, 10 parts
sodium dichromate, 1 part
5 minutes at 339 K (150° F)

↓

Rinse - tap water
2 minutes

↓

Dry - oven
30 minutes at 341 (155° F)

Ti-6Al-4V titanium alloy

↓

Degrease - acetone

↓

Alkaline clean -
15 minutes at 355 K (180° F)

↓

Rinse - hot tap water

↓

Pickle - 48% hydrofluoric acid,
30 kg/m^3 (4 oz/gal)
70% nitric acid,
337 kg/m^3 (45 oz/gal)
2 minutes at room temperature

↓

Rinse - tap water

↓

Phosphate fluoride treatment -
trisodium phosphate,
48.7 kg/m^3 (6.5 oz/gal)
potassium fluoride,
18.7 kg/m^3 (2.5 oz/gal)
hydrofluoric acid,
16.5 kg/m^3 (2.2 oz/gal)
2 minutes at room temperature

↓

Soak - deionized water
15 minutes at 341 K (155° F)

↓

Rinse - deionized water
1 minute at room temperature

↓

Dry - forced warm air

High Strength Bolts

Boron/aluminum or
Ti-6Al-4V titanium alloy

↓

All panel parts acetone cleaned

APPENDIX C

BUCLASP2 MODELS

The BUCLASP2 computer program (ref. 4) was used to calculate the minimum buckling load for some of the skin-stringer panels listed in table I. The two BUCLASP2 models used in these analyses are shown in figure 17. One model simulated the diffusion-bonded, adhesive-bonded, and brazed skin-stringer attachment methods. The other model simulated the spotwelded attachment method. Both models were simply supported along the edges, which is consistent with the panel test conditions, and consisted of an assembly of flat-plate elements with curved-plate elements at the corners of the hat-shaped stringer. The darkened areas of the skin and the stringer flanges indicate the portions of the cross section that were rigidly connected in the analysis. These areas cover the entire flange width in model 1 and the spotweld nugget diameter for model 2. In each analysis, the attachment area was continuous over the length of the model; therefore, the effect of spotweld spacing on buckling load was not determined by the BUCLASP2 program.

Two other differences exist between the test specimens and configurations of the analytical models. In the analytical model, the model width is the distance between the simple supports. The test specimens, however, had 12.7 mm (0.5 in.) of skin material beyond the simple supports. To account for the additional material in the analytical determination of the buckling loads, an additional load was obtained by multiplying the analytically determined load per unit width in the elements at the edge of the model by 12.7 mm (0.5 in.). This additional load was added to the buckling load given in the BUCLASP2 output.

An additional geometric difference exists between the end boundary conditions of the analytical models and the test specimens. Because the ends of the test specimens are embedded in potting compound, the specimens have boundary conditions nearly equivalent to fixed-end boundary conditions. In contrast, BUCLASP2 only provides for boundary conditions of models with simply supported ends. Proper analytical buckling loads were obtained from the BUCLASP2 analysis, however, by using an analytical model length that produced mode shapes similar to those observed on the test specimens. All test specimens generally exhibited the same buckling pattern; therefore, model 1 and specimen C-4 were arbitrarily chosen to determine the model length that produces the correct mode shape. The results from this analysis are shown in figure 18 where buckling load is plotted as a function of model length for specimen C-4. The curve indicates that buckling load is independent of model length over the range of analytical model lengths investigated. In addition, cross-sectional distortion over these model lengths does not change and corresponds closely with the observed experimental mode shape. Therefore, a model length of 254 mm (10 in.) was chosen for the analysis.

The BUCLASP2 program analyzes the structure by using a longitudinal strain distributed uniformly over the cross section. This is consistent with the method of loading the test specimens.

APPENDIX C

Input Data

Dimensional input data for the cross section of each analytical model are given in table I. Material property input data for each specimen are given in tables III and IV. The data given for Young's modulus in table IV were obtained from the strain gages on the panels. The Young's modulus of the boron/aluminum composite material in the eutectically bonded stringers (E-1 to E-6) and the Borsic/aluminum stringers (H-12 to H-17) is higher than the Young's modulus of the boron/aluminum composite material in the cold-formed (C-3 to C-7) and hot-formed (H-3 to H-7) stringers due to an approximately 6 percent greater fiber volume fraction.

Analytical Results

Buckling loads obtained by using the BUCLASP2 program and the material property data given in table III are much higher than the buckling loads determined experimentally from the strain gage data. These analytically determined buckling loads and the associated longitudinal strains and half-wave numbers (n) of the buckle pattern are given in table IV for a panel length of 254 mm (10 in.). The experimental buckling loads are given in table II. The difference between the analytical and experimental buckling loads is attributable to nonlinear effects caused by initial imperfections and/or material plasticity. Examination of the strain gage data indicates that the longitudinal strains are within the elastic limits of the panel materials prior to buckling. Thus, longitudinal plasticity does not contribute to panel buckling. The mode shapes obtained from BUCLASP2 analysis and from failed panels indicate that a high degree of transverse bending takes place in the corner radii of the hat-shaped stringer which are adjacent to the skin. (See fig. 19.) Since the composite material exhibits plastic behavior in the transverse direction at a very low level of strain (approximately 0.001, see ref. 6), transverse plasticity in the corner radii of the hat-shaped stringer probably affected the buckling behavior of the panels.

In order to determine the magnitude of the effect of this transverse plasticity, the transverse tangent modulus of the corner elements adjacent to the skin was arbitrarily assumed to be 10 GPa (1.5×10^6 psi) instead of 131 GPa (19×10^6 psi) (the tangent modulus at a strain level of approximately 0.002) and the panels were analyzed again using BUCLASP2. The buckling-load results from these analyses are shown in figure 8 and tabulated in table IV. Comparison of the predictions in table IV indicates a 26-percent lower buckling load is calculated from this lower transverse modulus. Thus, transverse plasticity significantly reduces the buckling load. Therefore, plastic buckling solutions should be used cautiously when predicting buckling loads for structures using this unidirectional laminate material.

REFERENCES

1. Royster, Dick M.; Wiant, H. Ross; and Bales, Thomas T.: Joining and Fabrication of Metal-Matrix Composite Materials. NASA TM X-3282, 1975.

2. Standard for Metric Practice. E 380-76, American Soc. Testing & Mater., 1976.

3. Progar, Donald J.; and St. Clair, Terry: Preliminary Evaluation of a Novel Polyimide Adhesive for Bonding Titanium and Reinforced Composites. Materials Review '75, Volume 7 of National SAMPE Technical Conference Series, Soc. Advance. Mater. & Process Eng., 1975, pp. 53-67.

4. Tripp, L. L.; Tamekuni, M.; and Viswanathan, A. V.: User's Manual - BUCLASP2: A Computer Program for Instability Analysis of Biaxially Loaded Composite Stiffened Panels and Other Structures. NASA CR-112226, 1973.

5. Bales, Thomas T.; Wiant, H. Ross; and Royster, Dick M.: Brazed Borsic/Aluminum Structural Panels. NASA TM X-3432, 1977.

6. Herakovich, C. T.; Davis, J. G., Jr.; and Viswanathan, C. N.: Tensile and Compressive Behavior of Borsic/Aluminum. Composite Materials: Testing and Design (Fourth Conference), ASTM Spec. Tech. Publ. 617, 1977, pp. 344-357.

TABLE I.- DIMENSIONS OF SKIN-STRINGER PANELS

[The following panel dimensions were constant for each panel: length - 248.9 mm, W - 152.4 mm, w - 139.7 mm, r_a - 6.4 mm. See figure 3 for identification of symbols]

(a) SI units

Panel	Skin	Mass, kg	Area, cm^2	b_s, mm	b_w, mm	b_h, mm	t_s, mm	t_w, mm	Joining method	Spacing, mm
Boron/aluminum stringers fabricated by cold forming process										
C-1	Ti	0.490	4.103	101.6	39.6	39.1	1.351	1.351	Fastener	50.8
C-3	B/Al	.308	4.723	102.4	37.1	40.4	1.679	1.402	Spotweld	19.0
C-4	B/Al	.308	4.716	101.3	37.3	38.9	1.671	1.326	Diffusion bond	Continuous
C-5	Ti	.364	4.206	102.1	37.3	38.4	1.321	1.389	Spotweld	19.0
C-6	Ti	.372	4.277	102.4	37.1	37.8	1.351	1.313	Diffusion bond	Continuous
C-7	Ti	.359	4.168	101.8	36.8	39.4	1.295	1.318	Adhesive bond	Continuous
Boron/aluminum stringers fabricated by hot forming process										
H-1	B/Al	0.439	4.742	103.6	37.6	40.6	1.687	1.460	Fastener	50.8
H-3	B/Al	.315	4.832	103.4	40.1	39.6	1.679	1.333	Diffusion bond	Continuous
H-4	B/Al	.309	4.723	102.6	37.8	40.1	1.666	1.351	Adhesive bond	Continuous
H-5	Ti	.360	4.148	102.9	37.8	40.1	1.341	1.364	Spotweld	19.0
H-6	B/Al	.311	4.761	101.3	38.1	40.9	1.692	1.356	Spotweld	19.0
H-7	Ti	.372	4.290	103.1	37.8	40.1	1.331	1.331	Diffusion bond	Continuous
Boron/aluminum stringers fabricated by eutectic bonding process										
E-1	B/Al	0.301	4.619	105.7	38.1	42.7	1.694	1.247	Spotweld	19.0
E-2	Ti	.357	4.123	106.2	38.6	42.7	1.321	1.250	Spotweld	19.0
E-3	B/Al	.303	4.632	105.2	39.1	42.7	1.676	1.267	Diffusion bond	Continuous
E-4	Ti	.357	4.084	105.9	37.8	42.4	1.311	1.247	Diffusion bond	Continuous
E-5	B/Al	.302	4.613	105.7	39.4	42.4	1.661	1.247	Adhesive bond	Continuous
E-6	Ti	.353	4.077	103.4	38.3	42.7	1.300	1.250	Adhesive bond	Continuous
E-7	B/Al	.430	4.613	106.2	40.1	42.9	1.689	1.318	Fastener	50.8
E-8	Ti	.481	4.000	106.2	37.6	42.4	1.328	1.257	Fastener	50.8
Borsic/aluminum stringers fabricated by hot forming process										
H-12	Ti	0.356	4.026	102.6	38.3	40.1	1.341	1.260	Spotweld	19.0
H-13	Ti	.361	4.116	102.4	39.1	40.9	1.321	1.234	Braze	Continuous
H-14	Bsc/Al	.285	4.284	102.6	37.3	40.1	1.598	1.265	Spotweld	19.0
H-15	Ti	.364	4.123	102.6	37.8	40.4	1.346	1.219	Braze	Continuous
H-16	Bsc/Al	.295	4.413	101.3	38.1	39.9	1.590	1.224	Braze	Continuous
H-17	Bsc/Al	.298	4.477	102.4	40.1	40.1	1.610	1.219	Braze	Continuous

TABLE I.- Concluded

[The following panel dimensions were constant for each panel: length - 9.8 in., W - 6.0 in., w - 5.5 in., r_a - 0.25 in. See figure 3 for identification of symbols]

(b) U.S. Customary Units

Panel	Skin	Mass, lbm	Area, in^2	b_s, in.	b_w, in.	b_h, in.	t_s, in.	t_w, in.	Joining method	Spacing, in.
Boron/aluminum stringers fabricated by cold forming process										
C-1	Ti	1.080	0.636	4.00	1.56	1.54	0.0532	0.0532	Fastener	2.0
C-3	B/Al	.678	.732	4.03	1.46	1.59	.0661	.0552	Spotweld	.75
C-4	B/Al	.680	.731	3.99	1.47	1.53	.0658	.0522	Diffusion bond	Continuous
C-5	Ti	.802	.652	4.02	1.47	1.51	.0520	.0547	Spotweld	.75
C-6	Ti	.821	.663	4.03	1.46	1.49	.0532	.0517	Diffusion bond	Continuous
C-7	Ti	.792	.646	4.01	1.45	1.55	.0510	.0519	Adhesive bond	Continuous
Boron/aluminum stringers fabricated by hot forming process										
H-1	B/Al	0.968	0.735	4.08	1.48	1.60	0.0664	0.0575	Fastener	2.0
H-3	B/Al	.694	.749	4.07	1.58	1.56	.0661	.0525	Diffusion bond	Continuous
H-4	B/Al	.682	.732	4.04	1.49	1.58	.0656	.0532	Adhesive bond	Continuous
H-5	Ti	.793	.643	4.05	1.49	1.58	.0528	.0537	Spotweld	.75
H-6	B/Al	.686	.738	3.99	1.50	1.61	.0666	.0534	Spotweld	.75
H-7	Ti	.821	.665	4.06	1.49	1.58	.0524	.0524	Diffusion bond	Continuous
Boron/aluminum stringers fabricated by eutectic bonding process										
E-1	B/Al	0.663	0.716	4.16	1.50	1.68	0.0667	0.0491	Spotweld	0.75
E-2	Ti	.788	.639	4.18	1.52	1.68	.0520	.0492	Spotweld	.75
E-3	B/Al	.668	.718	4.14	1.54	1.68	.0660	.0499	Diffusion bond	Continuous
E-4	Ti	.787	.633	4.17	1.49	1.67	.0516	.0491	Diffusion bond	Continuous
E-5	B/Al	.666	.715	4.16	1.55	1.67	.0654	.0491	Adhesive bond	Continuous
E-6	Ti	.779	.632	4.07	1.51	1.68	.0512	.0492	Adhesive bond	Continuous
E-7	B/Al	.948	.715	4.18	1.58	1.69	.0665	.0519	Fastener	2.0
E-8	Ti	1.060	.620	4.18	1.48	1.67	.0523	.0495	Fastener	2.0
Borsic/aluminum stringers fabricated by hot forming process										
H-12	Ti	0.785	0.624	4.04	1.51	1.58	0.0528	0.0496	Spotweld	0.75
H-13	Ti	.795	.638	4.03	1.54	1.61	.0520	.0486	Braze	Continuous
H-14	Bsc/Al	.628	.664	4.04	1.47	1.58	.0629	.0498	Spotweld	.75
H-15	Ti	.803	.639	4.04	1.49	1.59	.0530	.0480	Braze	Continuous
H-16	Bsc/Al	.650	.684	3.99	1.50	1.57	.0626	.0482	Braze	Continuous
H-17	Bsc/Al	.656	.694	4.03	1.58	1.58	.0634	.0480	Braze	Continuous

TABLE II.- SKIN-STRINGER COMPRESSION PANEL DATA

(a) SI Units

Panel	Maximum load, kN	Average maximum stress, MPa	Buckling load, kN	Average buckling stress, MPa	Average strain at buckling $\bar{\epsilon}$, mm/mm
Boron/aluminum skin to boron/aluminum stringer - spotweld					
H-6	222.5	467.4	200.7	421.5	0.00185
C-3	224.7	475.8	203.4	430.8	.00182
E-1	188.6	408.4	133.3	288.5	.00117
Boron/aluminum skin to boron/aluminum stringer - high strength bolts					
H-1	221.7	467.5	219.8	463.5	0.00215
E-7	189.6	411.1	183.1	397.0	.00182
Boron/aluminum skin to boron/aluminum stringer - diffusion bond					
H-3	290.0	600.2	290.0	600.2	0.00286
C-4	304.5	645.8	289.0	612.7	.00284
E-3	239.3	516.6	209.2	451.5	.00202
Boron/aluminum skin to boron/aluminum stringer - adhesive bond					
H-4	284.0	601.3	276.0	584.4	0.00276
E-5	226.0	490.0	172.5	374.0	.00156
Titanium skin to boron/aluminum stringer - spotweld					
H-5	194.2	468.1	154.5	372.5	0.00205
C-5	176.2	418.8	127.9	304.1	.00173
E-2	154.5	374.9	123.5	299.6	.00157
Titanium skin to boron/aluminum stringer - high strength bolts					
C-1	189.4	461.7	140.6	342.7	0.00192
E-8	134.7	336.7	130.9	327.2	.00192
Titanium skin to boron/aluminum stringer - diffusion bond					
H-7	198.7	463.3	194.8	454.2	0.00275
C-6	226.4	529.3	222.5	520.2	.00314
E-4	200.1	490.0	195.0	477.6	.00275
Titanium skin to boron/aluminum stringer - adhesive bond					
C-7	213.2	511.5	213.2	511.5	0.00310
E-6	170.8	419.0	170.8	419.0	.00242

TABLE II.- Continued

(a) Concluded

Panel	Maximum load, kN	Average maximum stress, MPa	Buckling load, kN	Average buckling stress, MPa	Average strain at buckling $\bar{\epsilon}$, mm/mm
Borsic/aluminum skin to Borsic/aluminum stringer - spotweld					
H-14	185.4	432.9	161.9	377.9	0.00147
Borsic/aluminum skin to Borsic/aluminum stringer - braze sheet					
H-16	198.7	450.4	175.7	398.2	0.00161
Borsic/aluminum skin to Borsic/aluminum stringer - brazing foil					
H-17	210.4	470.0	205.8	459.6	0.00199
Titanium skin to Borsic/aluminum stringer - spotweld					
H-12	147.7	366.8	124.6	309.6	0.00174
Titanium skin to Borsic/aluminum stringer - brazing foil					
H-13	163.2	396.6	160.2	389.1	0.00225
Titanium skin to Borsic/aluminum stringer - braze sheet					
H-15	183.3	444.7	183.3	444.7	0.00259

TABLE II.- Continued

(b) U.S. Customary Units

Panel	Maximum load, lbf	Average maximum stress, psi	Buckling load, lbf	Average buckling stress, psi	Average strain at buckling $\bar{\epsilon}$, in./in.
Boron/aluminum skin to boron/aluminum stringer - spotweld					
H-6	50 026	67 786	45 115	61 132	0.00185
C-3	50 508	69 000	45 735	62 480	.00182
E-1	42 406	59 226	29 963	41 848	.00117
Boron/aluminum skin to boron/aluminum stringer - high strength bolts					
H-1	49 835	67 803	49 406	67 219	0.00215
E-7	42 630	59 622	41 172	57 583	.00182
Boron/aluminum skin to boron/aluminum stringer - diffusion bond					
H-3	65 196	87 044	65 196	87 044	0.00286
C-4	68 465	93 659	64 961	88 866	.00284
E-3	53 796	74 925	47 020	65 488	.00202
Boron/aluminum skin to boron/aluminum stringer - adhesive bond					
H-4	63 836	87 208	62 039	84 753	0.00276
E-5	50 815	71 070	38 780	54 238	.00156
Titanium skin to boron/aluminum stringer - spotweld					
H-5	43 651	67 886	34 742	54 031	0.00205
C-5	39 600	60 736	28 753	44 100	.00173
E-2	34 742	54 369	27 762	43 446	.00157
Titanium skin to boron/aluminum stringer - high strength bolts					
C-1	42 587	66 961	31 608	49 698	0.00192
E-8	30 279	48 837	29 421	47 453	.00192
Titanium skin to boron/aluminum stringer - diffusion bond					
H-7	44 680	67 188	43 804	65 871	0.00275
C-6	50 900	76 772	50 024	75 451	.00314
E-4	44 986	71 068	43 847	69 269	.00275
Titanium skin to boron/aluminum stringer - adhesive bond					
C-7	47 921	74 181	47 921	74 181	0.00310
E-6	38 407	60 771	38 407	60 771	.00242

TABLE II.- Concluded

(b) Concluded

Panel	Maximum load, lbf	Average maximum stress, psi	Buckling load, lbf	Average buckling stress, psi	Average strain at buckling $\bar{\epsilon}$, in./in.
Borsic/aluminum skin to Borsic/aluminum stringer - spotweld					
H-14	41 687	62 781	36 391	54 806	0.00147
Borsic/aluminum skin to Borsic/aluminum stringer - braze sheet					
H-16	44 677	65 317	39 503	57 753	0.00161
Borsic/aluminum skin to Borsic/aluminum stringer - brazing foil					
H-17	47 307	68 166	46 255	66 650	0.00199
Titanium skin to Borsic/aluminum stringer - spotweld					
H-12	33 198	53 202	28 016	44 897	0.00174
Titanium skin to Borsic/aluminum stringer - brazing foil					
H-13	36 697	57 518	36 008	56 439	0.00225
Titanium skin to Borsic/aluminum stringer - braze sheet					
H-15	41 213	64 496	41 213	64 496	0.00259

TABLE III.- BUCLASP2 MATERIAL PROPERTY INPUTS

Titanium:	
Young's modulus	121.3 GPa (17.6×10^6 psi)
Shear modulus	46.7 GPa (6.77×10^6 psi)
Poisson ratio	0.30
Metal-matrix composite:	
Young's modulus - longitudinal[a]	(See table IV)
Young's modulus - transverse	131.0 GPa (19.0×10^6 psi)
Major Poisson ratio	0.26
Shear modulus	57.2 GPa (8.3×10^6 psi)

[a]Determined from panel test data.

TABLE IV.- BUCLASP2 PREDICTIONS

(a) SI Units

Panel	Analysis model	Young's modulus, GPa	Based on measured properties (a)			Based on lower Young's modulus in corners (b)		
			Strain at buckling, mm/mm	Buckling load, kN	Half-waves, n	Strain at buckling, mm/mm	Buckling load, kN	Half-waves, n
C-3	2	234	2.57×10^{-3}	292.7	5	2.13×10^{-3}	242.1	4
C-4	1	234	3.58	396.5	6	2.64	291.9	4
C-5	2	234	2.65	205.2	4	2.32	180.1	4
C-6	1	234	3.90	288.0	7	3.24	239.4	4
C-7	1	234	3.46	251.7	7	3.06	222.9	5
H-3	1	228	3.54×10^{-3}	390.0	6	2.64×10^{-3}	290.7	4
H-4	1	228	3.52	383.4	6	2.66	289.3	4
H-5	2	228	2.71	205.9	6	2.38	180.6	4
H-6	2	228	2.75	301.3	5	2.19	240.6	4
H-7	1	228	3.54	260.2	7	3.09	227.0	5
E-1	2	248	2.15×10^{-3}	250.8	4	1.79×10^{-3}	208.3	3
E-2	2	248	2.14	164.8	5	1.97	151.5	4
E-3	1	248	2.95	346.0	5	2.25	263.8	4
E-4	1	248	3.09	231.2	6	2.69	200.9	5
E-5	1	248	2.90	336.7	5	2.21	257.0	4
E-6	1	248	3.03	225.5	6	2.64	196.3	5
H-12	2	248	2.45×10^{-3}	187.7	4	2.17×10^{-3}	166.1	4
H-13	1	248	3.18	235.5	6	2.70	200.5	4
H-14	2	248	2.16	243.1	5	1.78	200.3	4
H-15	1	248	3.28	240.5	6	2.77	203.0	4
H-16	1	248	2.99	330.4	5	2.22	245.7	4
H-17	1	248	2.91	327.8	5	2.20	247.6	4

[a]BUCLASP2 data using material properties given in table III.

[b]BUCLASP2 data using material properties given in table III except Young's modulus = 10 GPa in corners of stringer adjacent to the skin.

TABLE IV.- Concluded

(b) U.S. Customary Units

Panel	Analysis model	Young's modulus, psi	Based on measured properties (a)			Based on lower Young's modulus in corners (b)		
			Strain at buckling, in./in.	Buckling load, lbf	Half-waves, n	Strain at buckling, in./in.	Buckling load, lbf	Half-waves, n
C-3	2	34×10^6	2.57×10^{-3}	65 800	5	2.13×10^{-3}	54 432	4
C-4	1	34	3.58	89 130	6	2.64	65 616	4
C-5	2	34	2.65	46 120	4	2.32	40 485	4
C-6	1	34	3.90	64 750	7	3.24	53 812	4
C-7	1	34	3.46	56 590	7	3.06	50 115	3
H-3	1	33×10^6	3.54×10^{-3}	87 680	6	2.64×10^{-3}	65 347	4
H-4	1	33	3.52	86 200	6	2.66	65 039	4
H-5	2	33	2.71	46 300	6	2.38	40 607	4
H-6	2	33	2.75	67 740	5	2.19	54 097	4
H-7	1	33	3.54	58 490	7	3.09	51 042	5
E-1	2	36×10^6	2.15×10^{-3}	56 380	4	1.79×10^{-3}	46 824	3
E-2	2	36	2.14	37 040	5	1.97	34 064	4
E-3	1	36	2.95	77 790	5	2.25	59 310	4
E-4	1	36	3.09	51 970	6	2.69	45 153	5
E-5	1	36	2.90	75 690	5	2.21	57 765	4
E-6	1	36	3.03	50 690	6	2.64	44 124	5
H-12	2	36×10^6	2.45×10^{-3}	42 200	4	2.17×10^{-3}	37 330	4
H-13	1	36	3.18	52 950	6	2.70	45 065	4
H-14	2	36	2.16	54 660	5	1.78	45 037	4
H-15	1	36	3.28	54 060	6	2.77	45 641	4
H-16	1	36	2.99	74 270	5	2.22	55 233	4
H-17	1	36	2.91	73 690	5	2.20	55 670	4

[a]BUCLASP2 data using material properties given in table III.

[b]BUCLASP2 data using material properties given in table III except Young's modulus = 1.5×10^6 psi in corners of stringer adjacent to the skin.

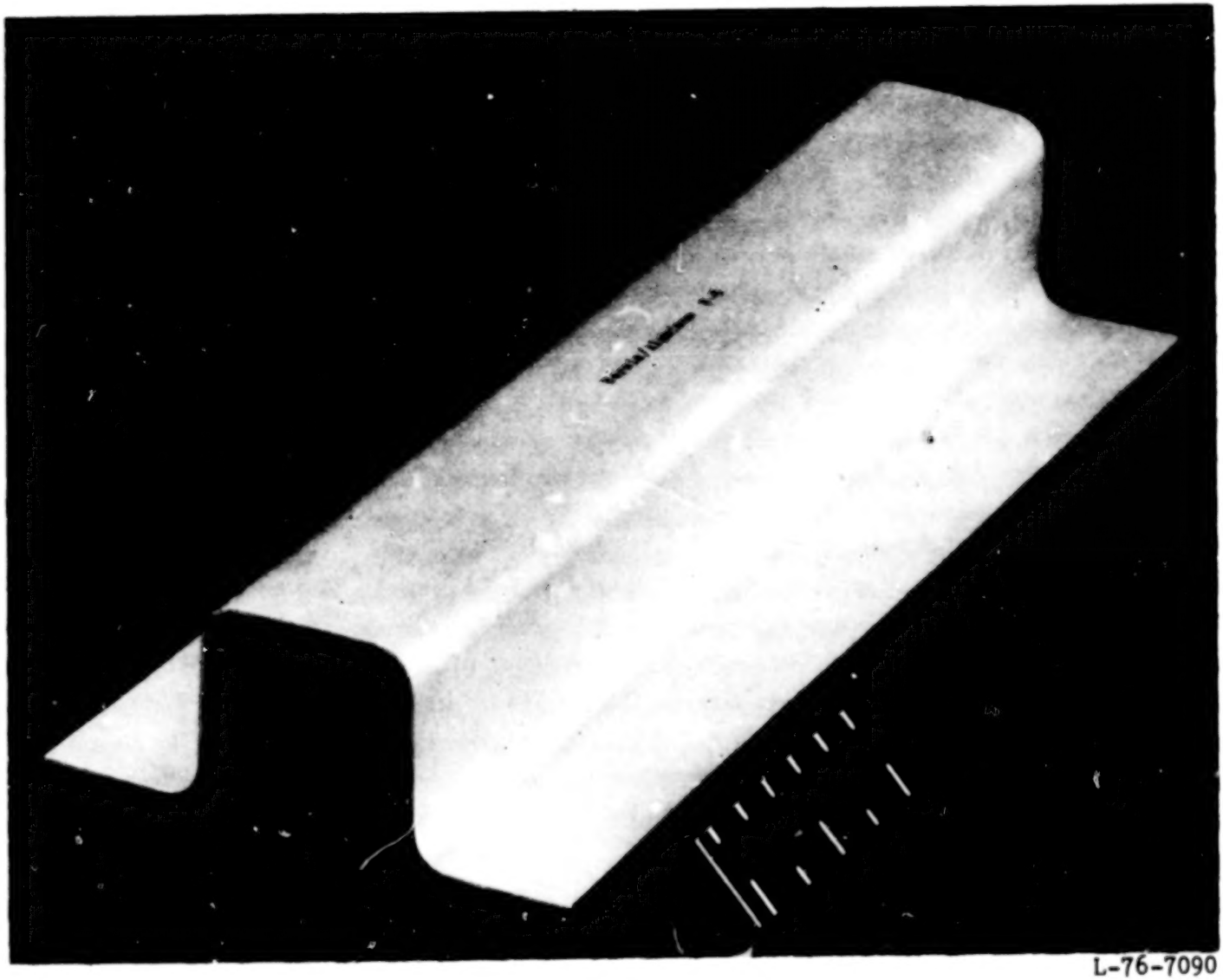

L-76-7090

Figure 1.- Borsic aluminum stringer.

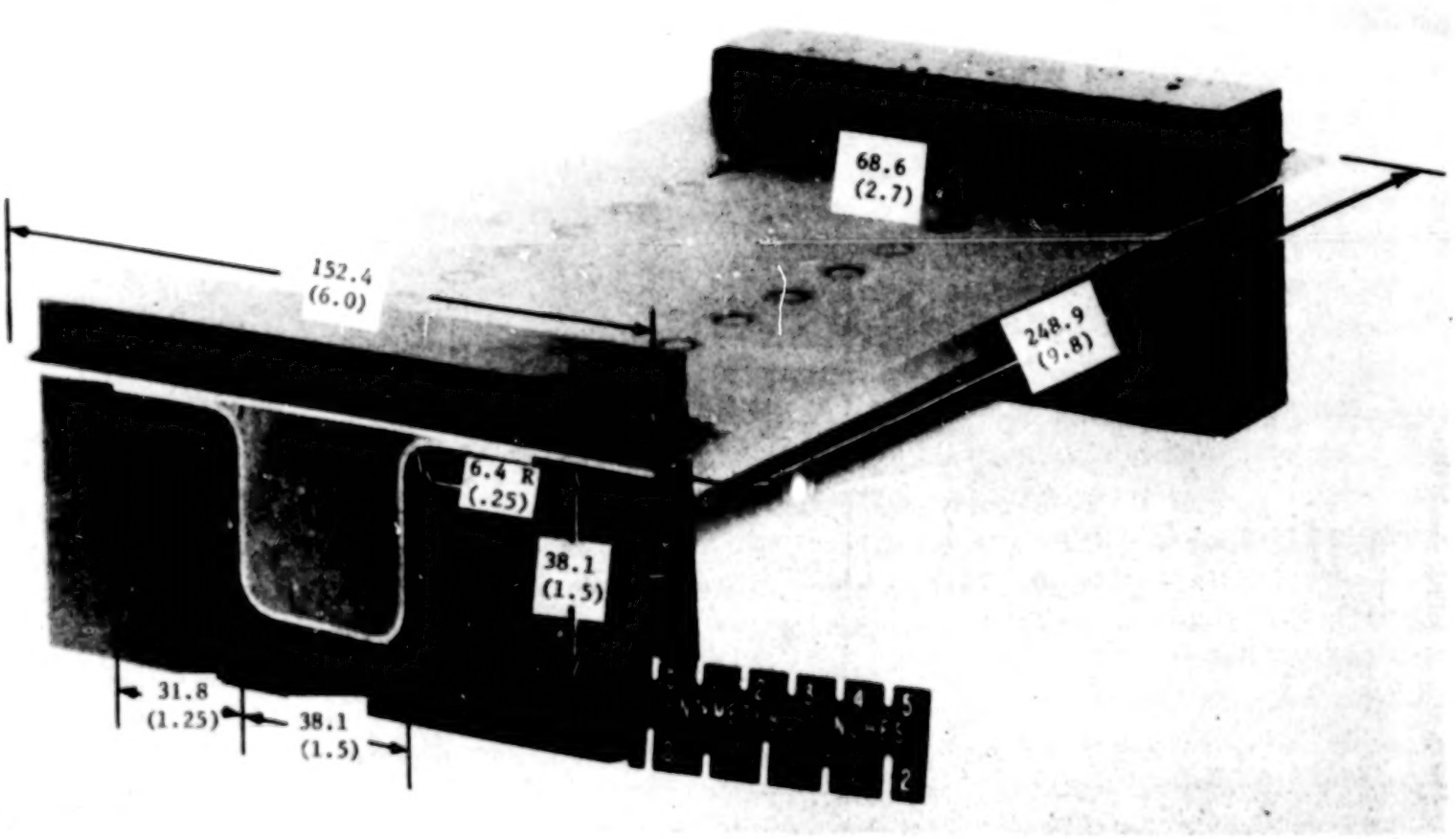

L-74-4367.1

Figure 2.- Skin-stringer panel. Dimensions are given in millimeters (inches).

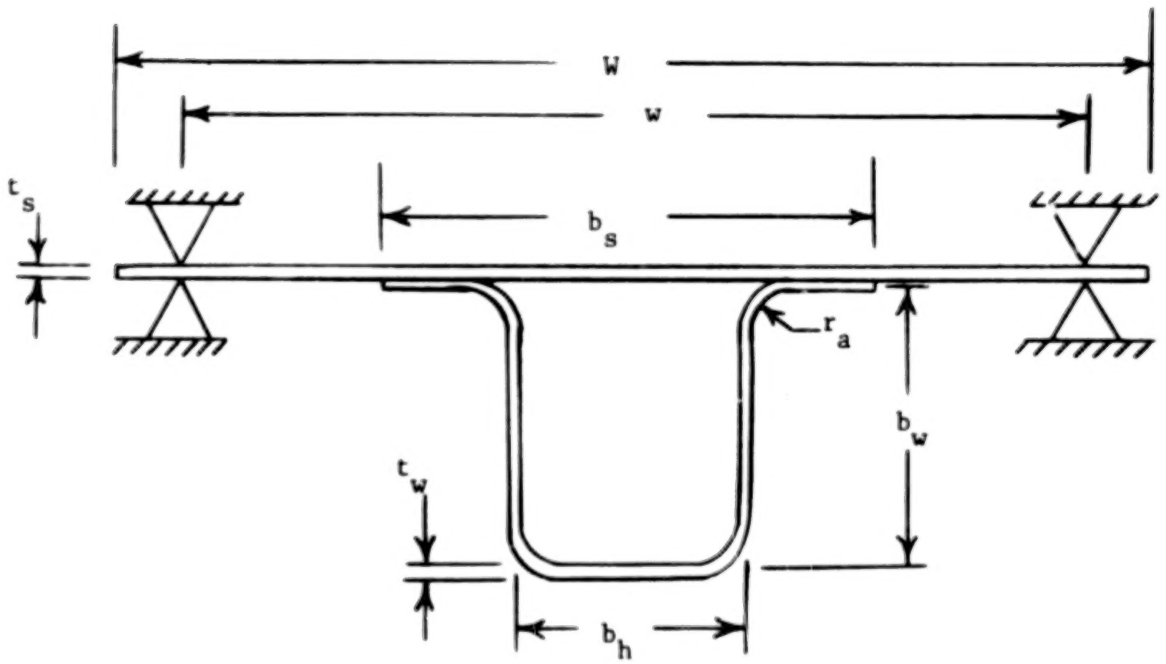

Figure 3.- Cross section of skin-stringer panel.

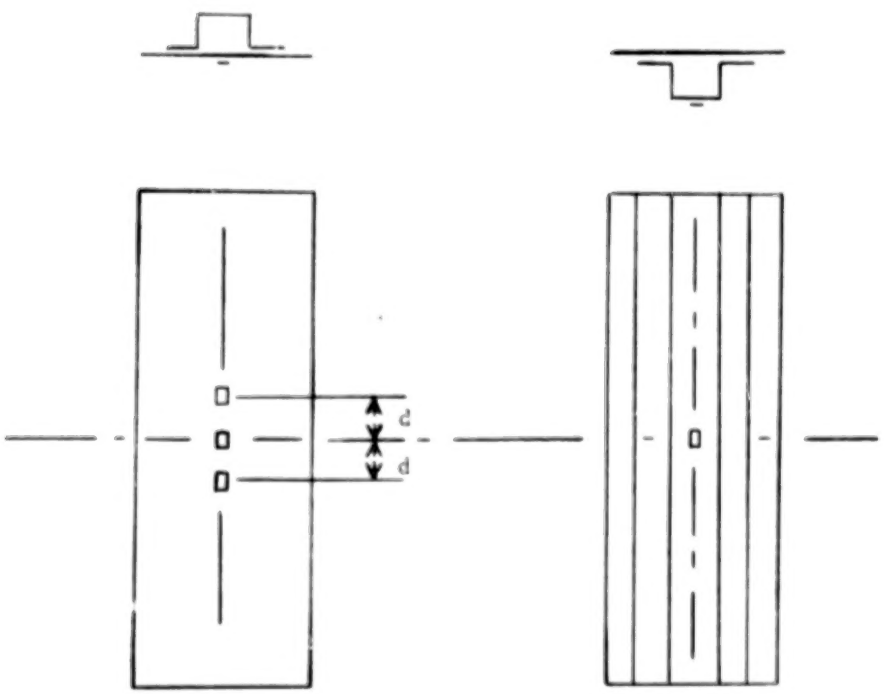

(a) Skin side. (b) Stringer side.

Figure 4.- Location of strain gages used in test of skin-stringer panels. d = 50.8 mm (2 in.).

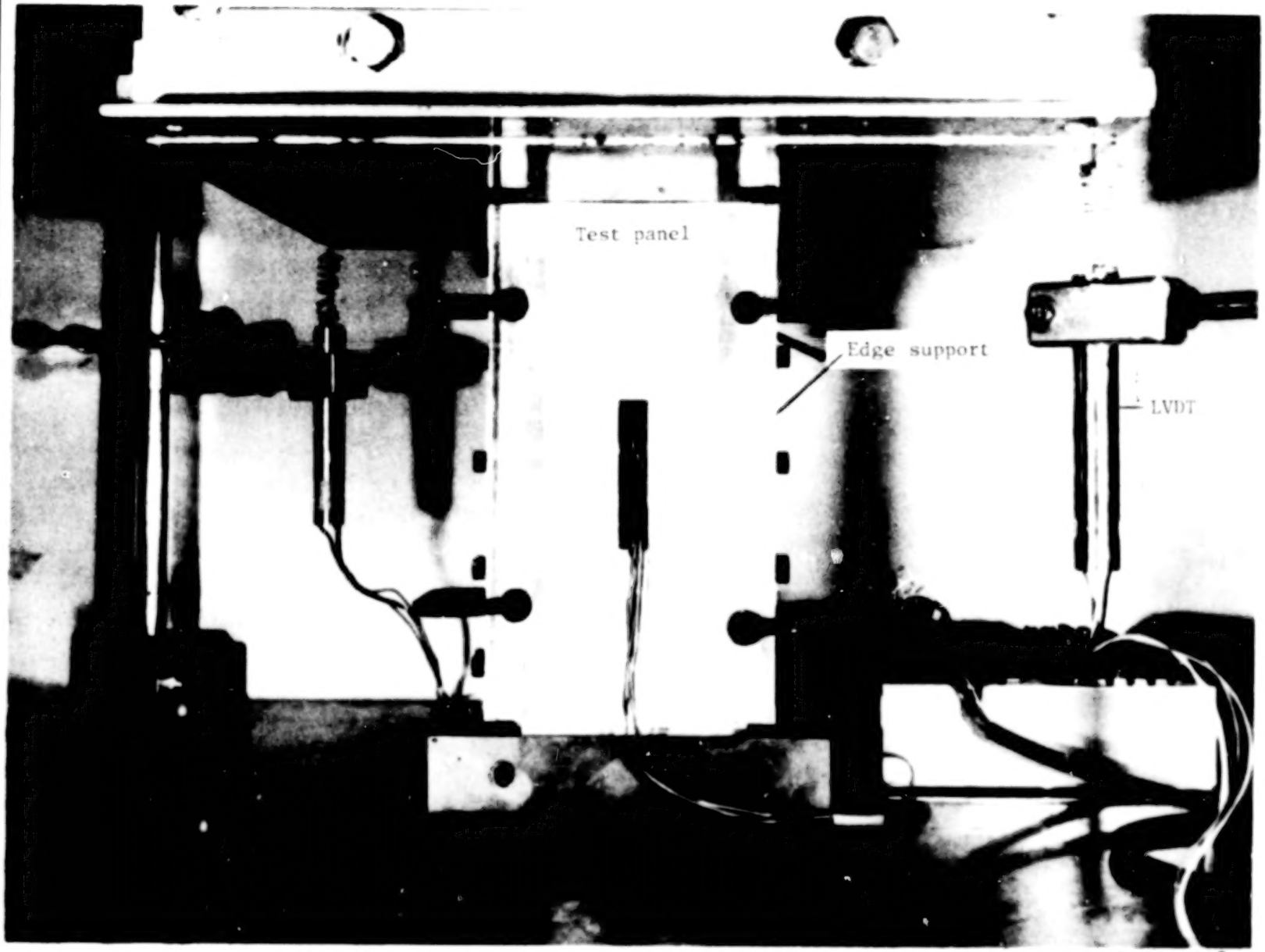

L-73-3038.1

Figure 5.- Test setup for skin-stringer panels.

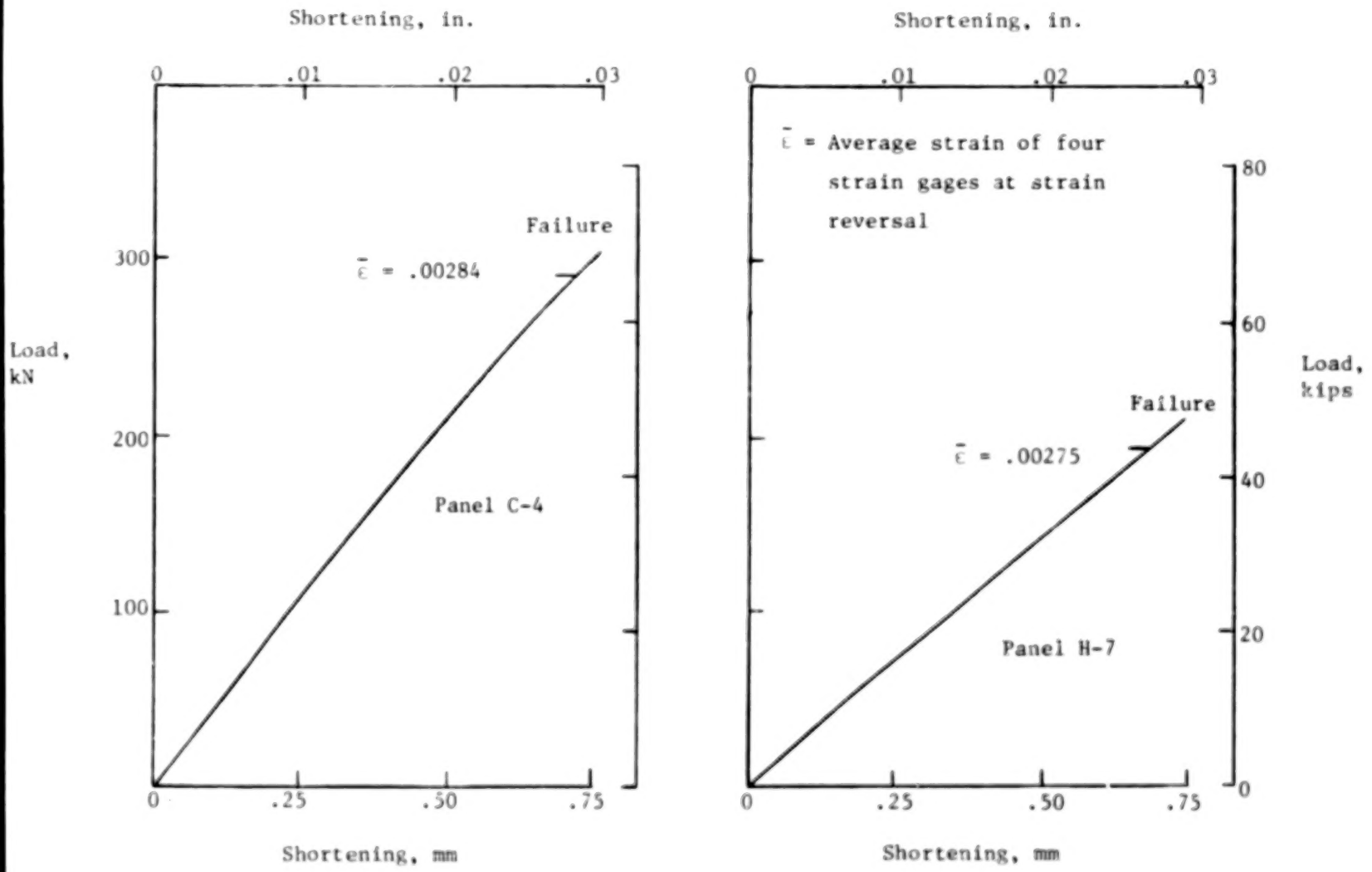

(a) B/Al skin.

(b) Ti skin.

Figure 6.- Typical LVDT load-shortening curves for skin-stringer panels.

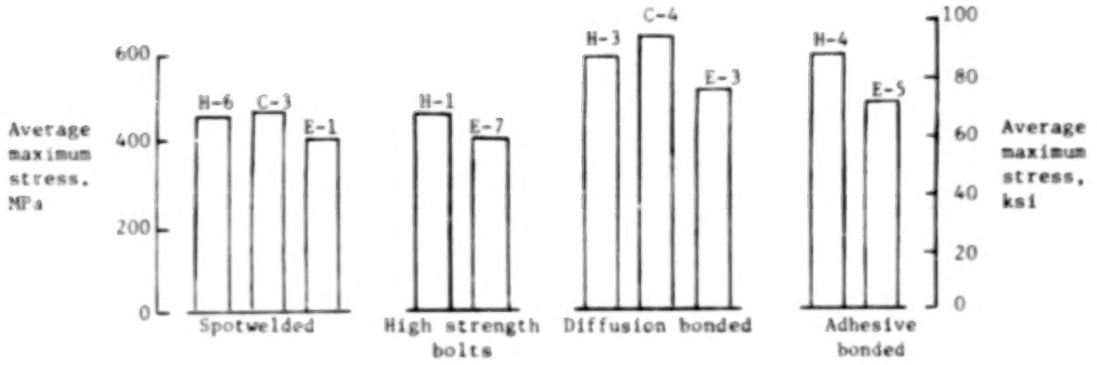

(a) B/Al skin - B/Al stringer.

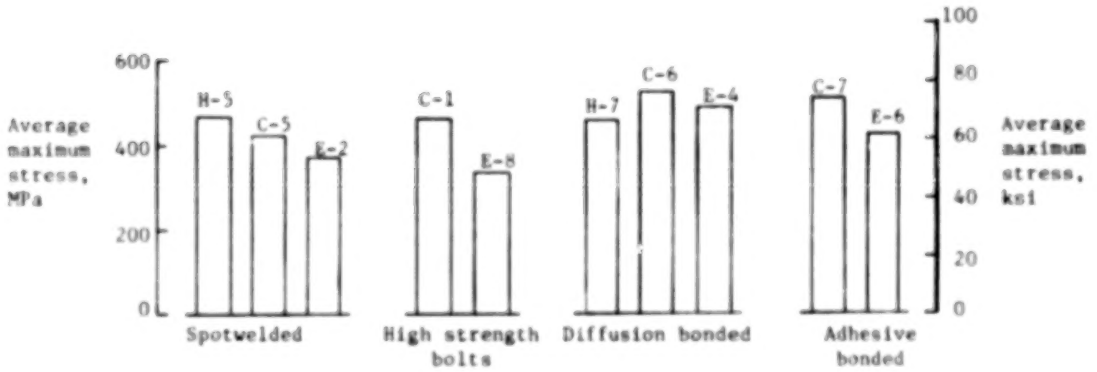

(b) Ti skin - B/Al stringer.

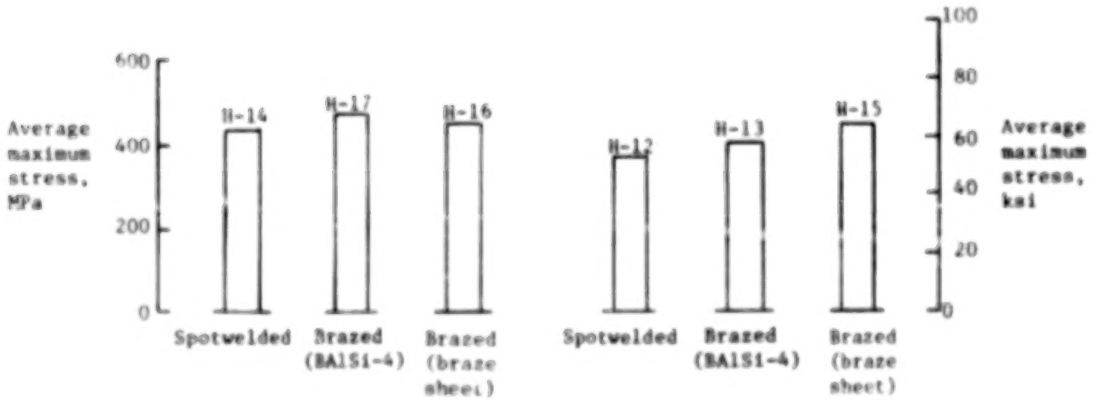

(c) Bsc/Al skin - Bsc/Al stringer. (d) Ti skin - Bsc/Al stringer.

Figure 7.- Average maximum stress of skin-stringer panels.
(See table I for panel identification.)

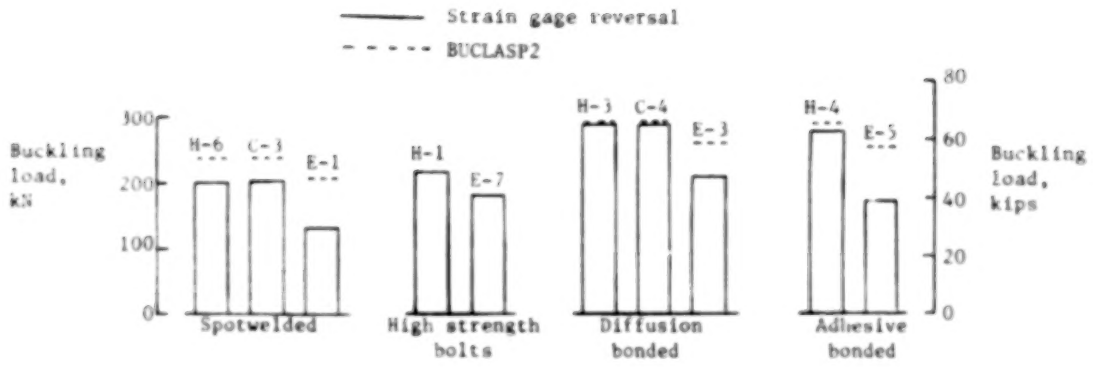

(a) B/Al skin - B/Al stringer.

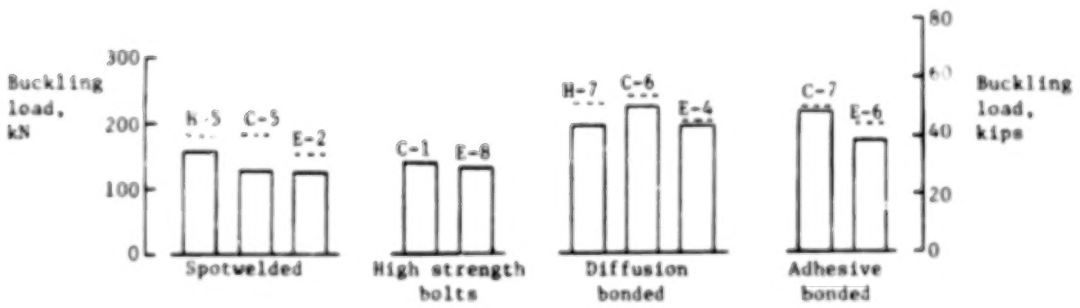

(b) Ti skin - B/Al stringer.

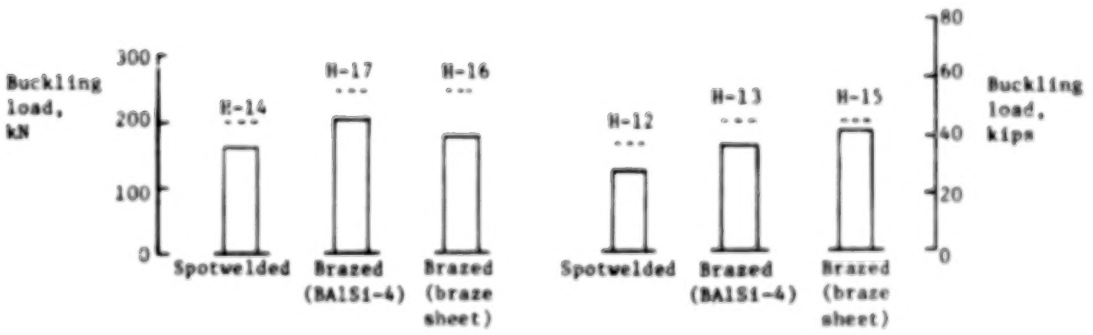

(c) Bsc/Al skin - Bsc/Al stringer.

(d) Ti skin - Bsc/Al stringer.

Figure 8.- Skin-stringer panel buckling loads.
(See table I for panel identification.)

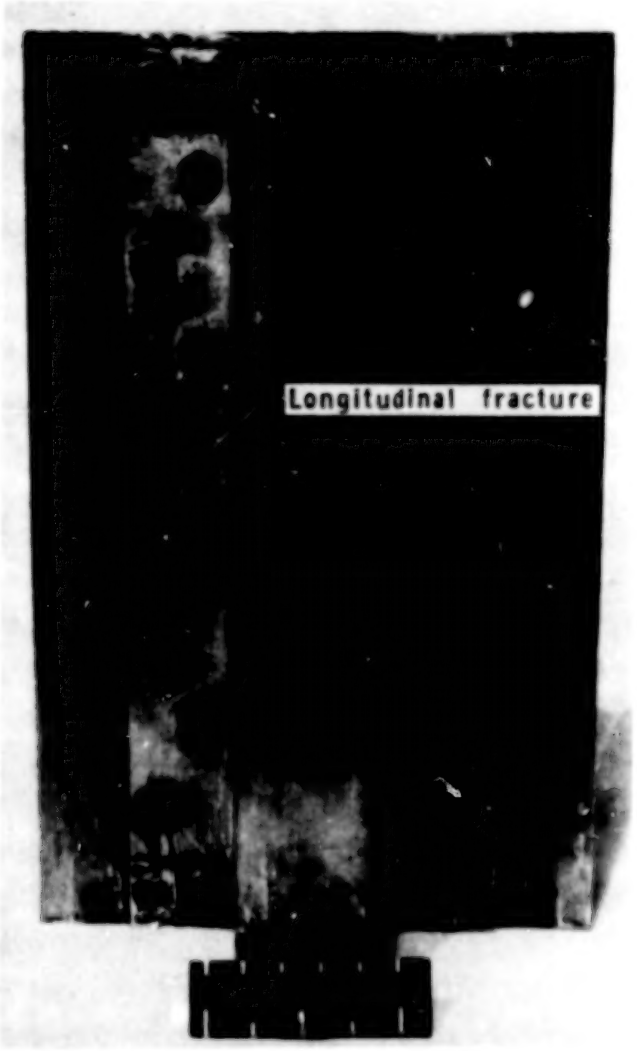

L-78-21

(a) Panel C-1 (mechanical fasteners - Ti skin).

Figure 9.- Typical failures of skin-stringer panels.

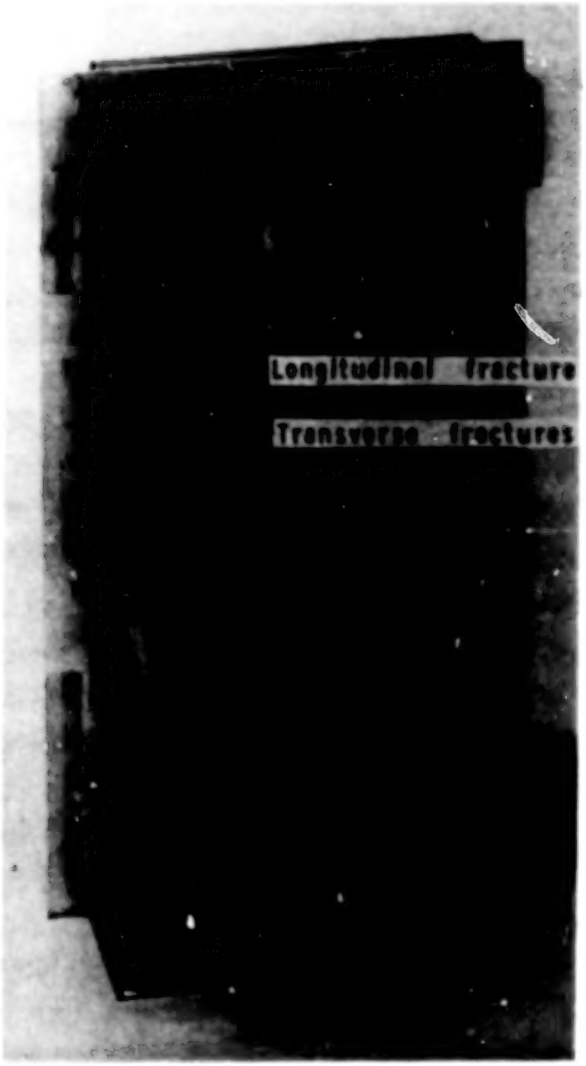

Stringer

L-78-22

(b) Panel C-6 (diffusion bonded - Ti skin).

Figure 9.- Continued.

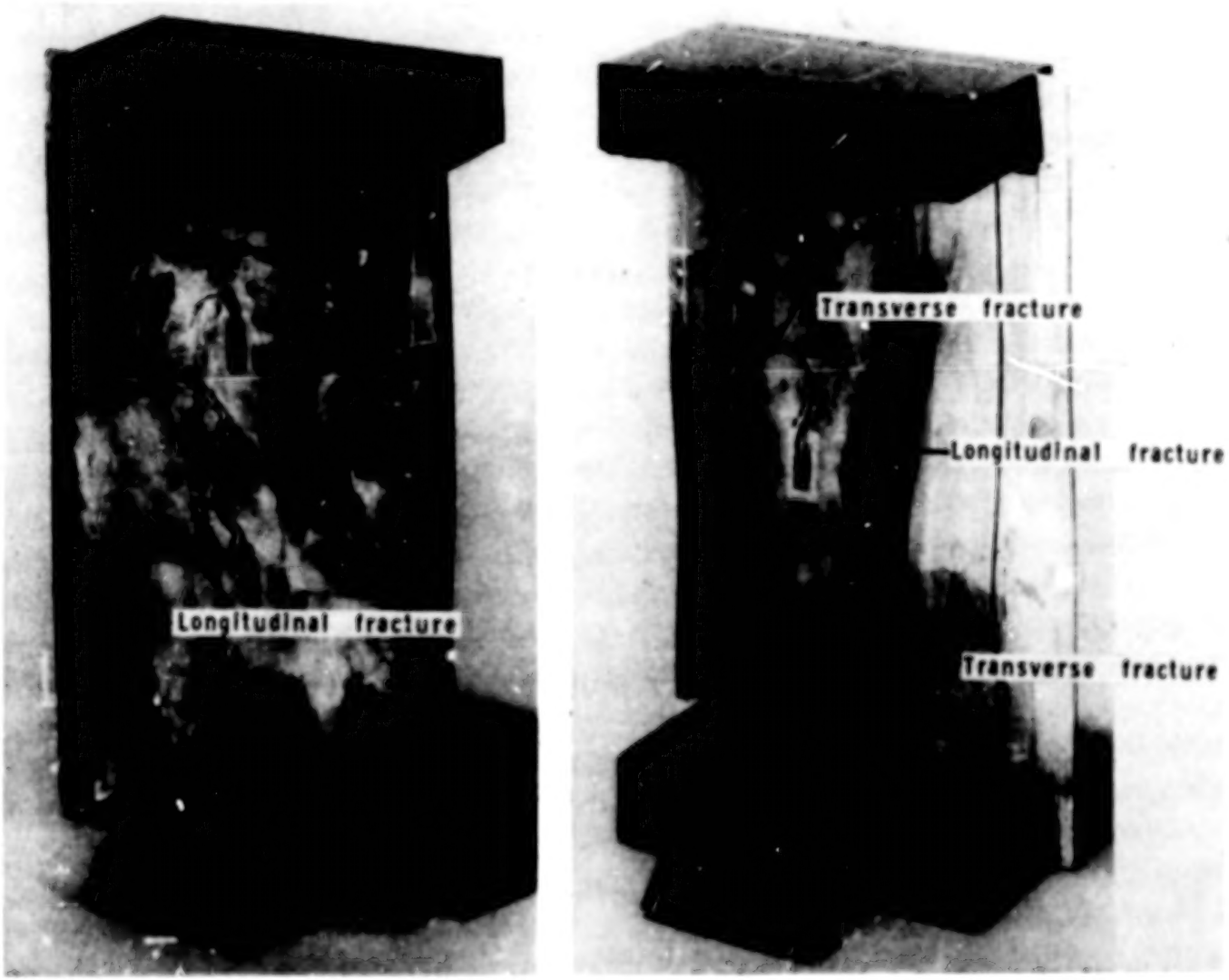

(c) Panel C-4 (diffusion bonded - B/Al skin).

Figure 9.- Continued.

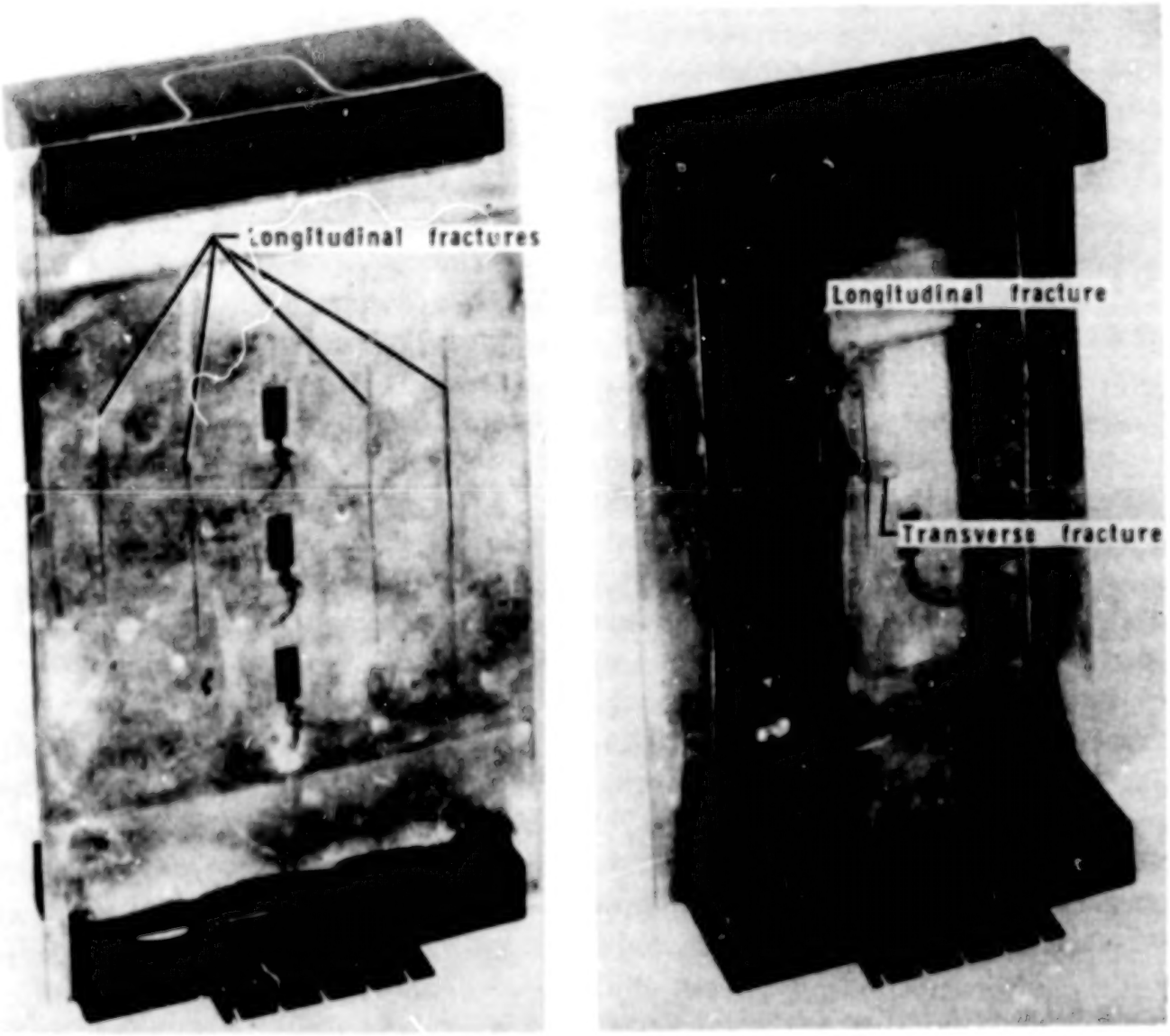

(d) Panel E-3 (diffusion bonded - B/Al skin).

Figure 9.- Continued.

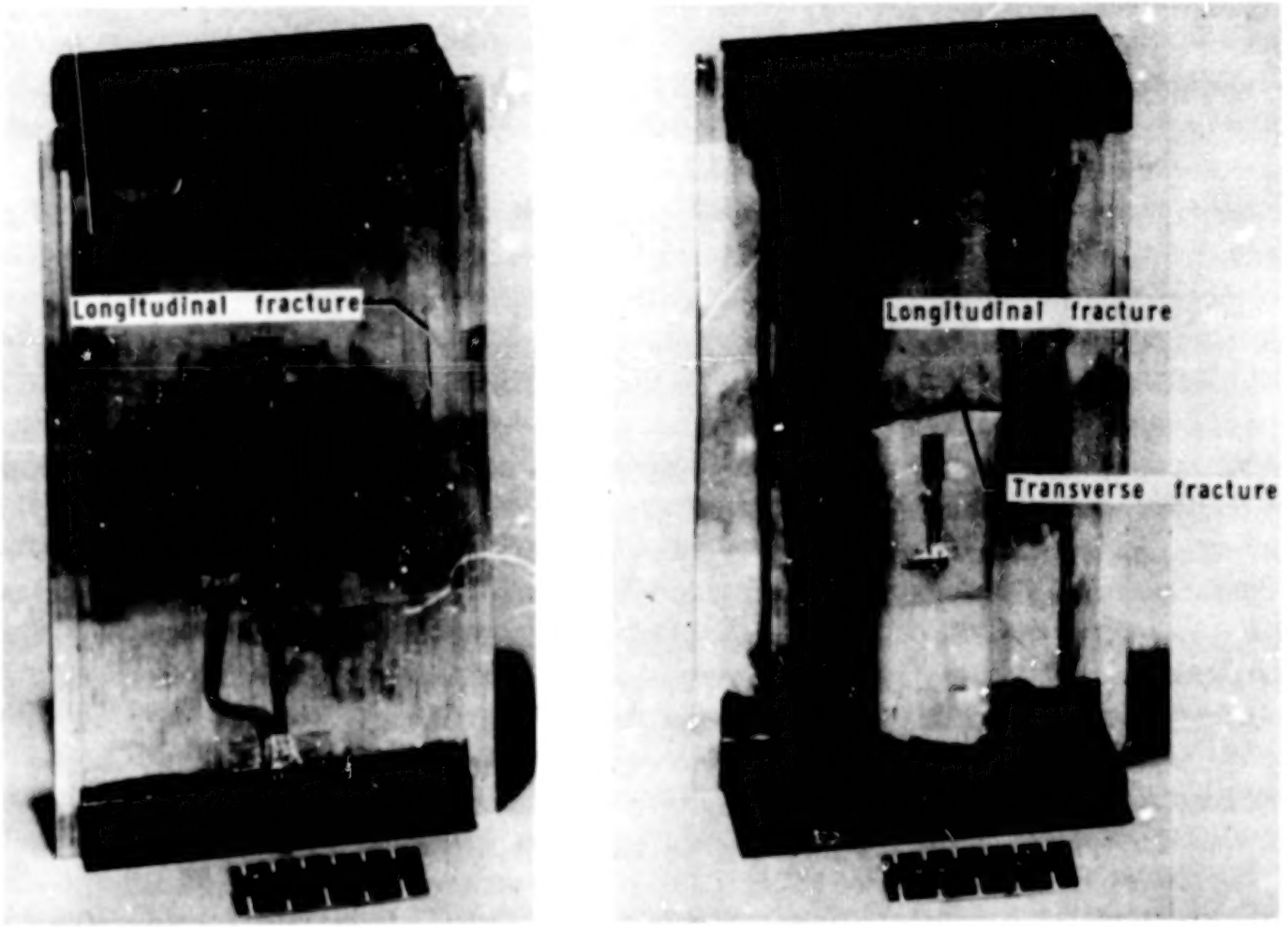

Skin

Stringer

L-78-25

(e) Panel H-4 (adhesive bonded - B/Al skin).

Figure 9.- Continued.

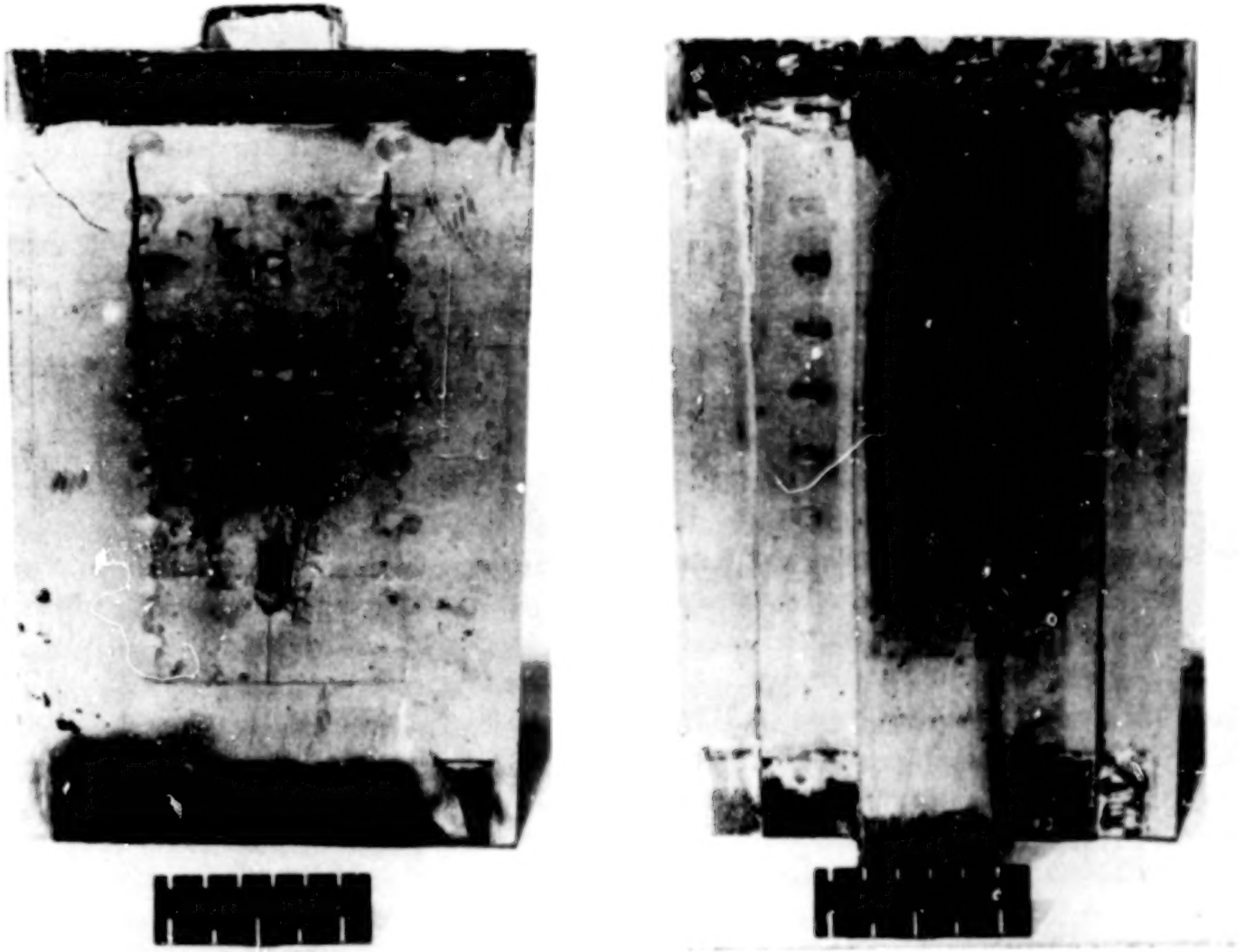

Skin

Stringer

L-78-26

(f) Panel H-14 (spotwelded - Bsc/Al skin).

Figure 9.- Continued.

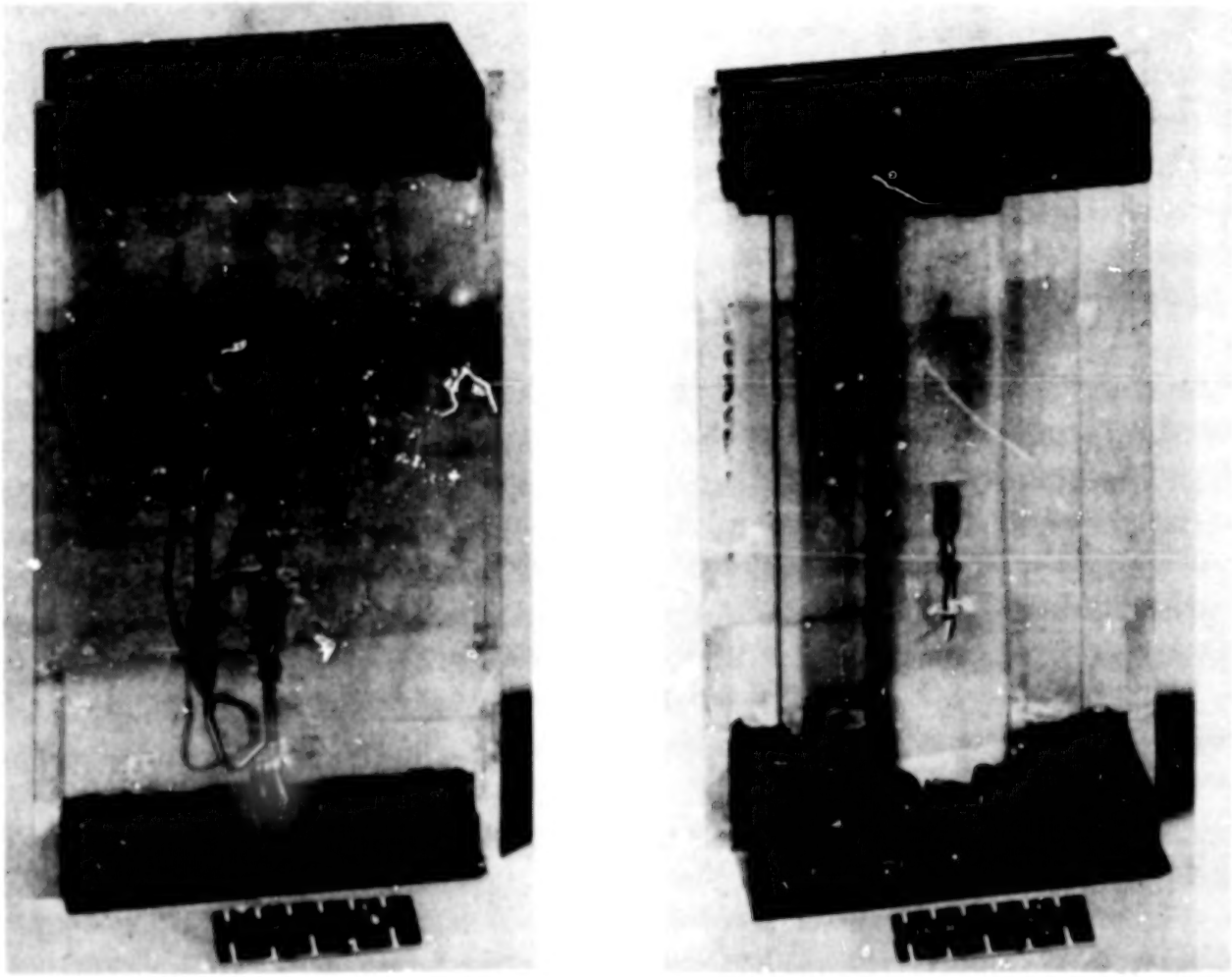

Skin Stringer

L-7[illegible]27

(g) Panel H-16 (brazed - Bsc/Al skin).

Figure 9.- Concluded.

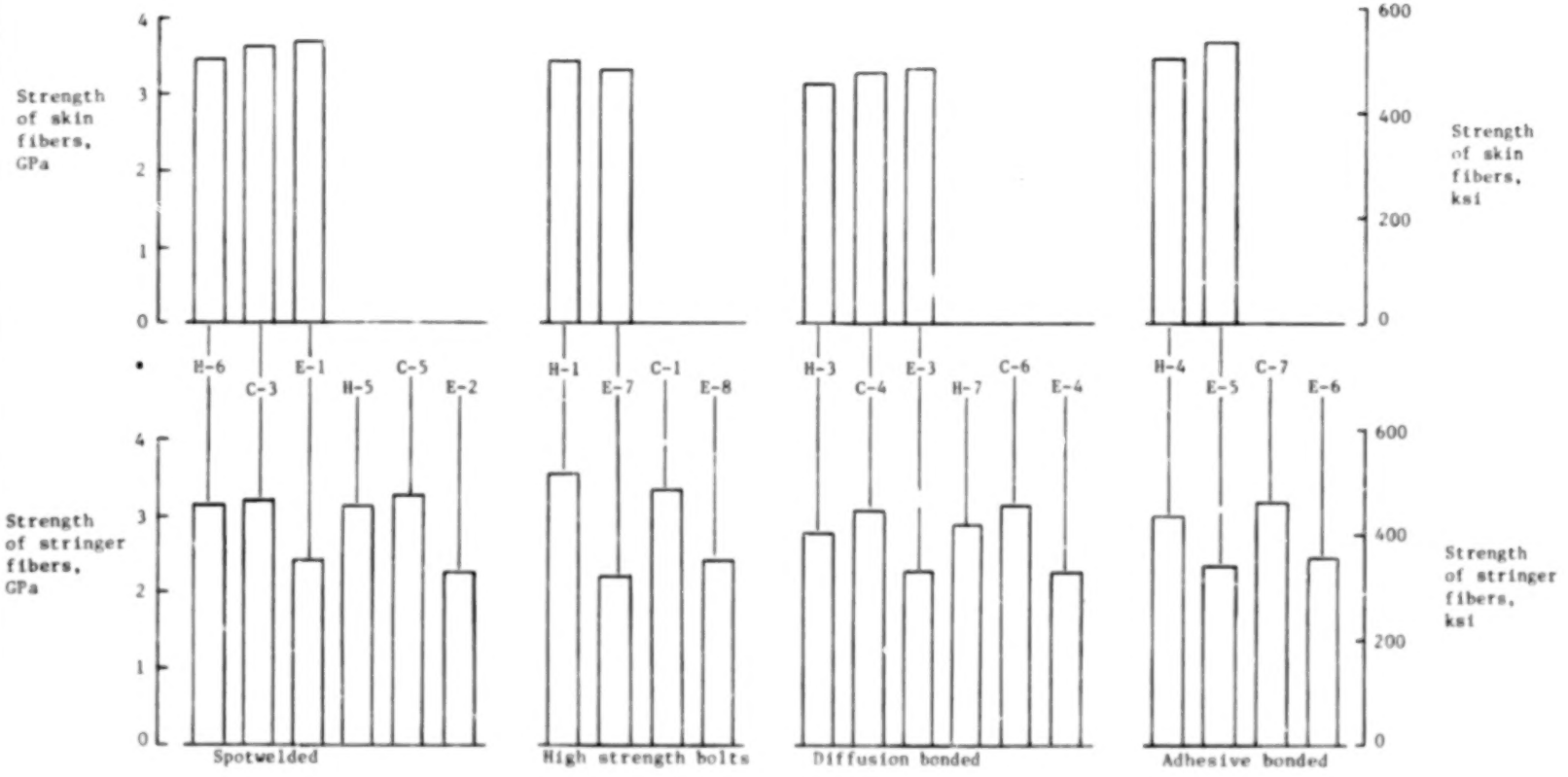

(a) Boron.

Figure 10.- Fiber bending strength. (See table I for panel identification.)

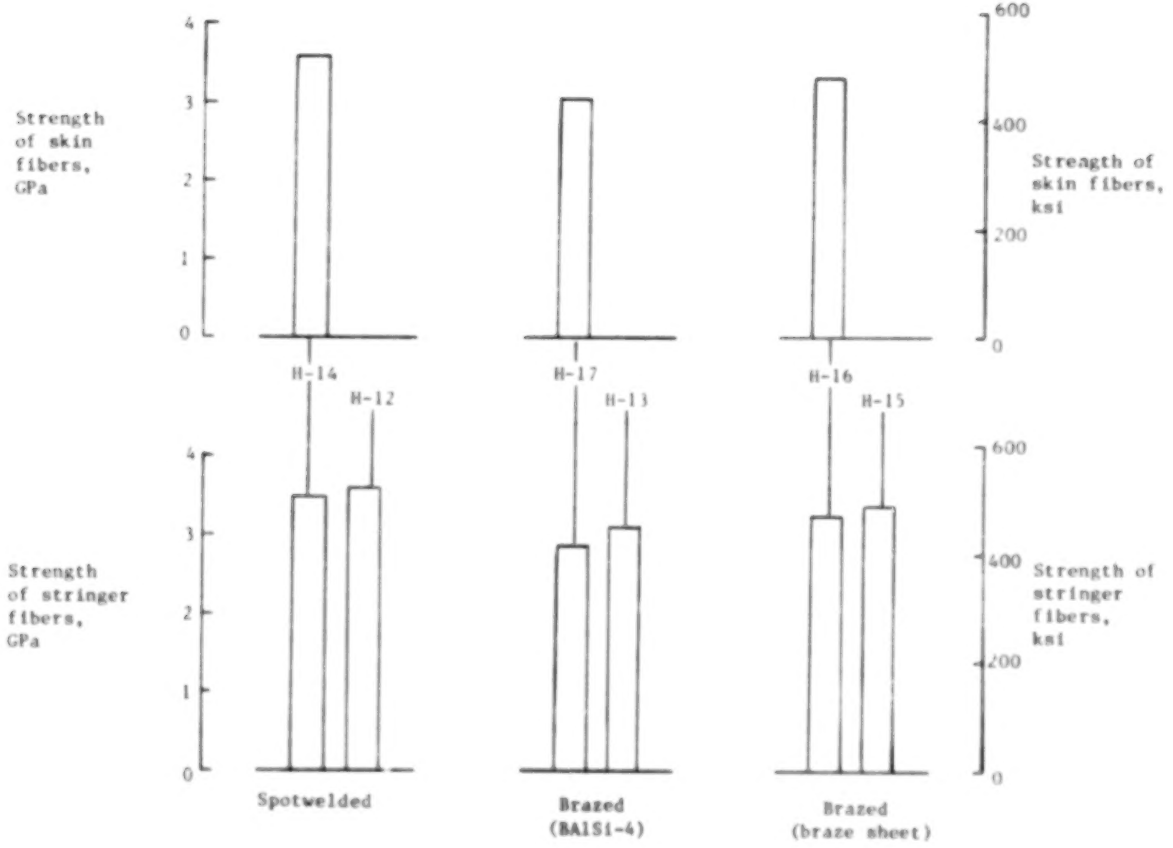

(b) Borsic.

Figure 10.- Concluded.

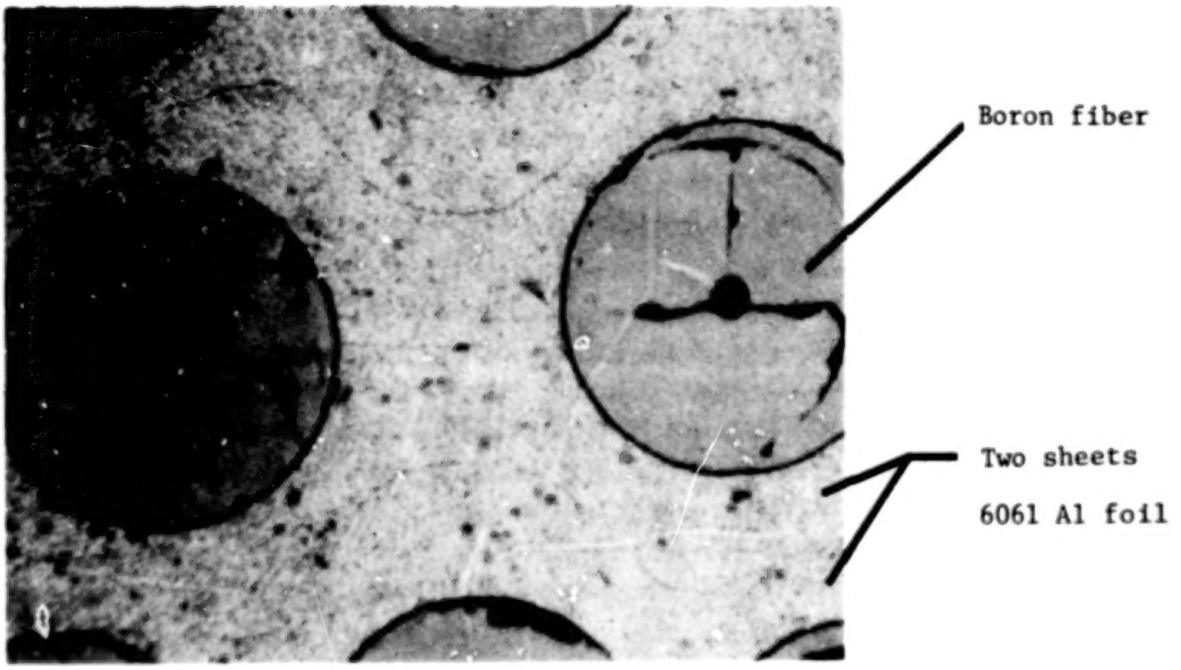

(a) Skin.

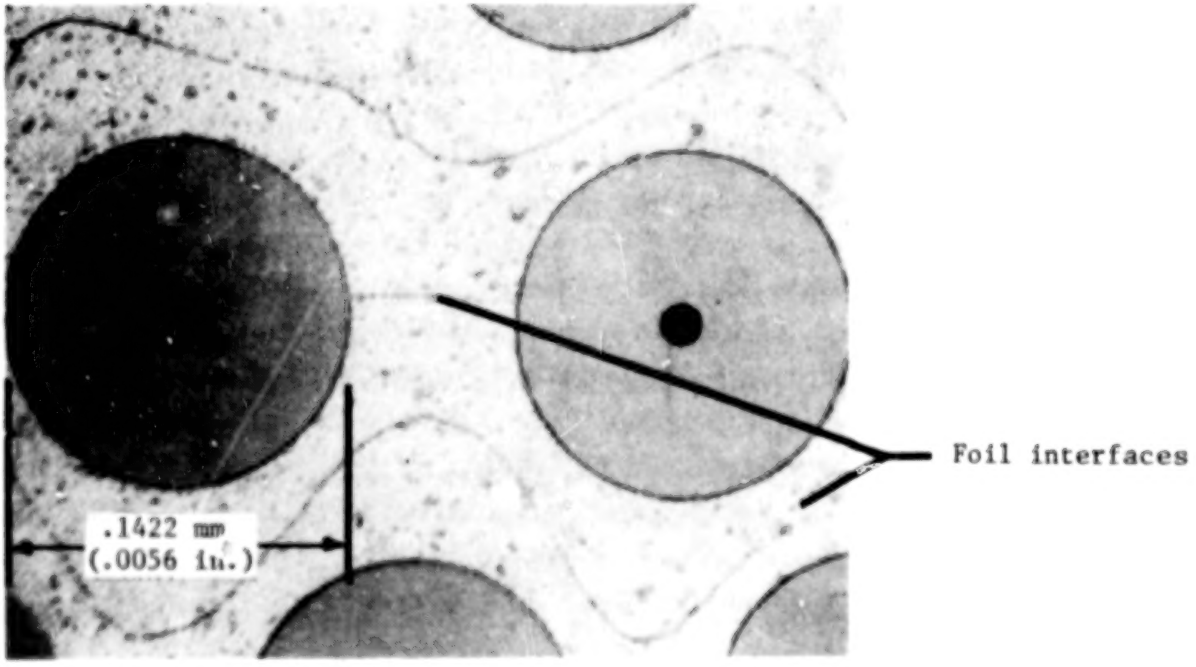

(b) Cold-formed stringer.

L-78-28

Figure 11.- Photomicrographs of "as received" panel parts.

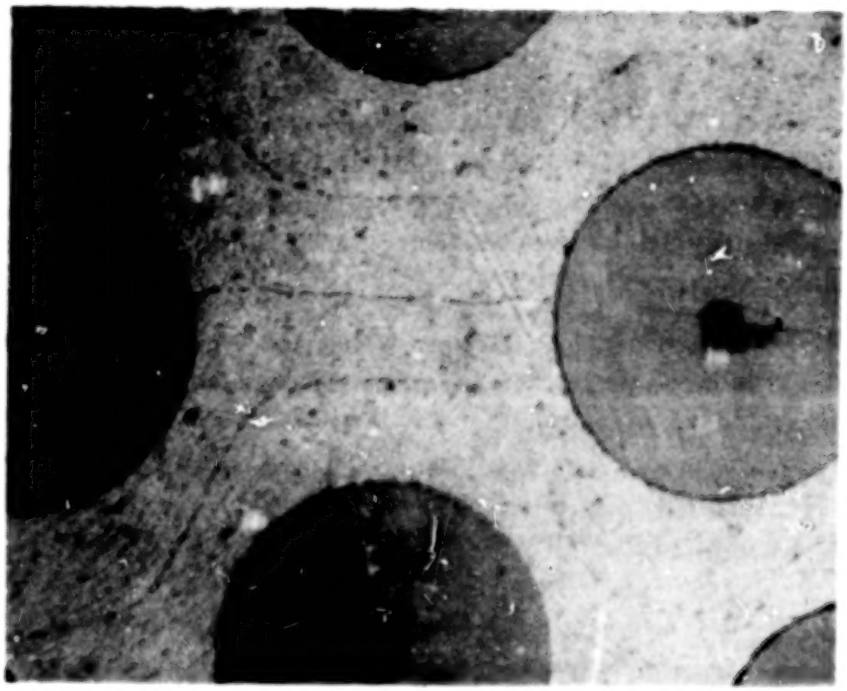

(c) Hot-formed stringer.

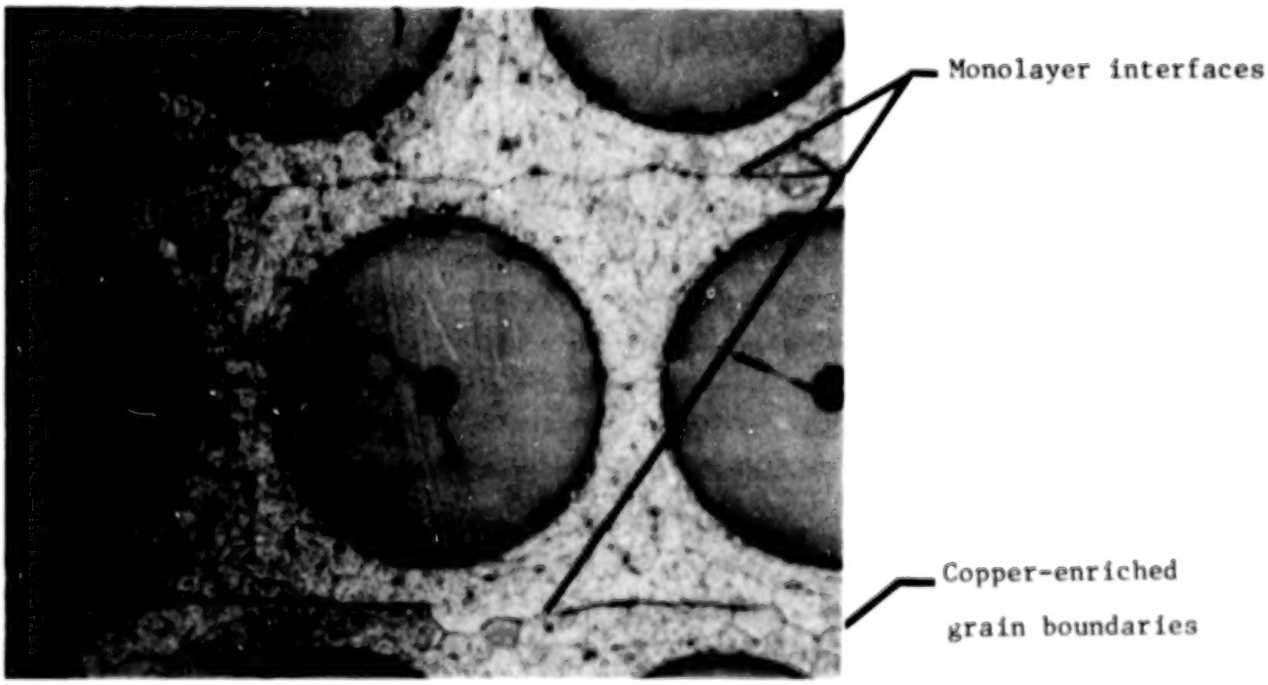

(d) Eutectically bonded stringer.

L-78-29

Figure 11.- Concluded.

(a) B/Al skin - B/Al stringer.

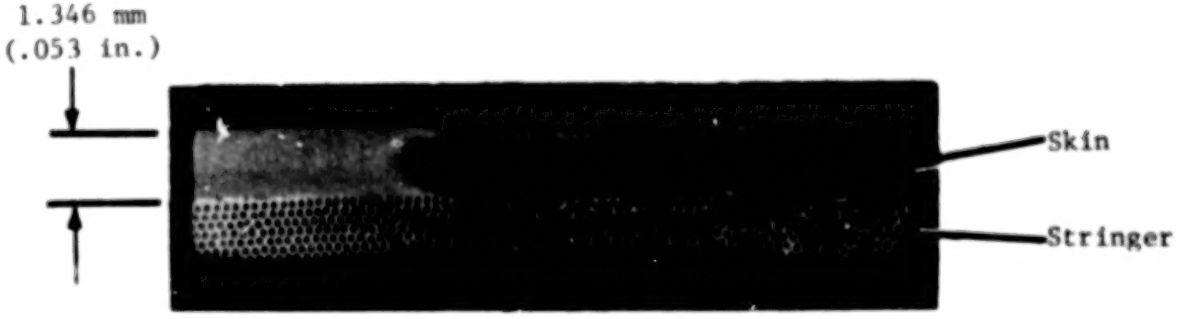

(b) Ti skin - B/Al stringer.

L-78-30

Figure 12.- Photomicrographs of typical resistance spotwelds.

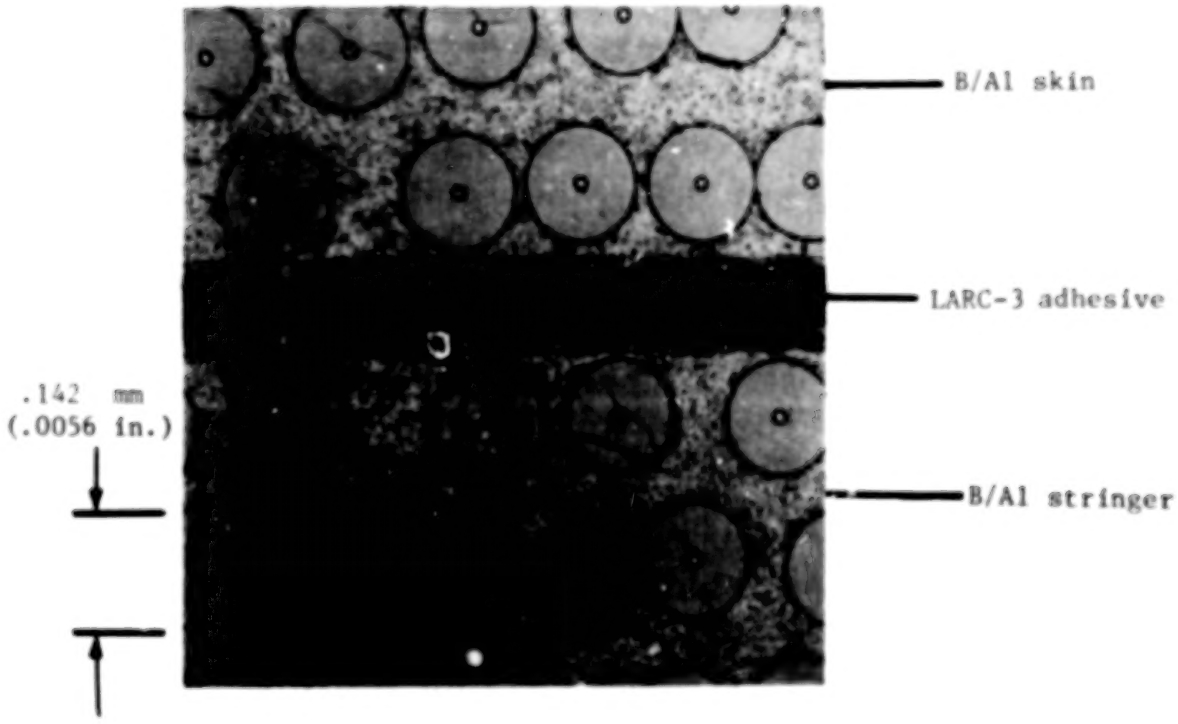

(a) Adhesive-bonded joint.

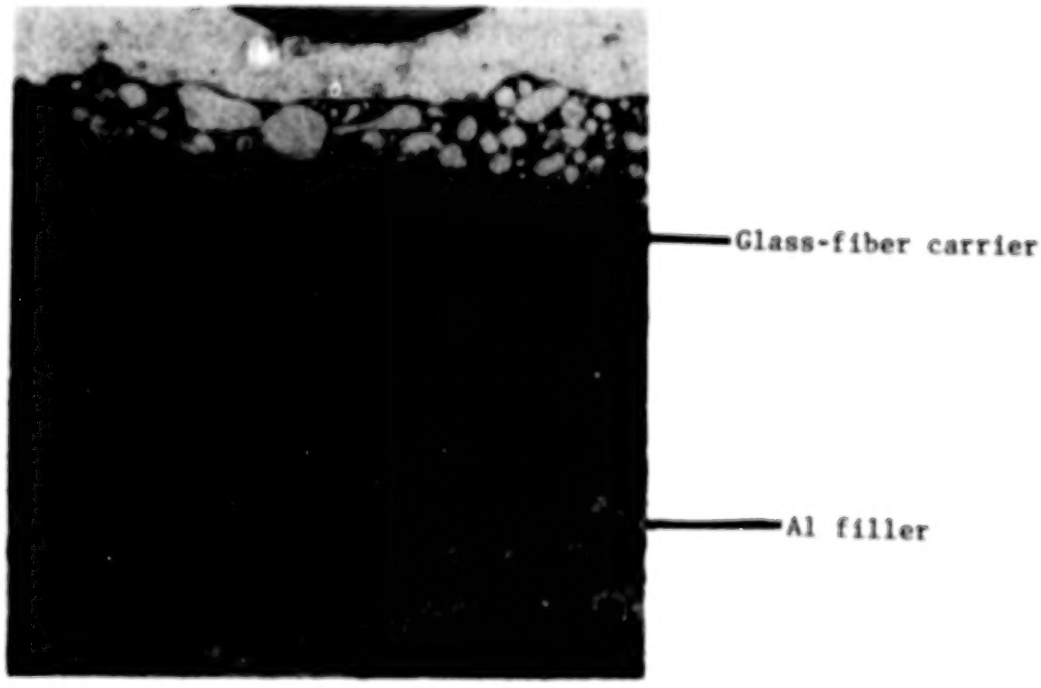

(b) Adhesive detail.

L-78-31

Figure 13.- Photomicrographs of LARC-3 adhesive bond.

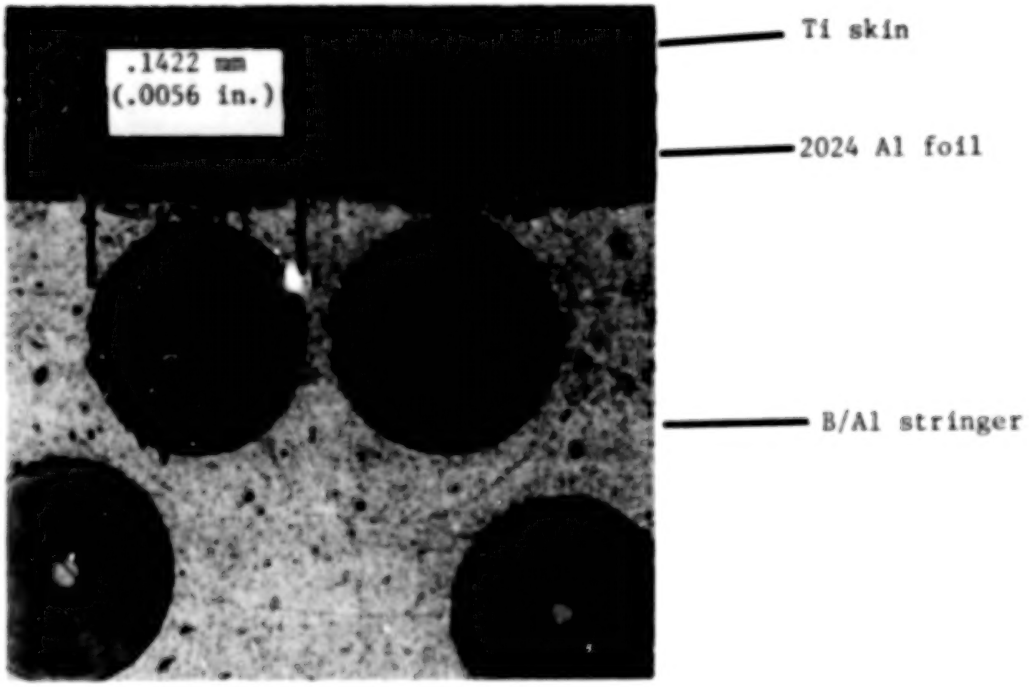

(a) Ti skin - B/Al stringer.

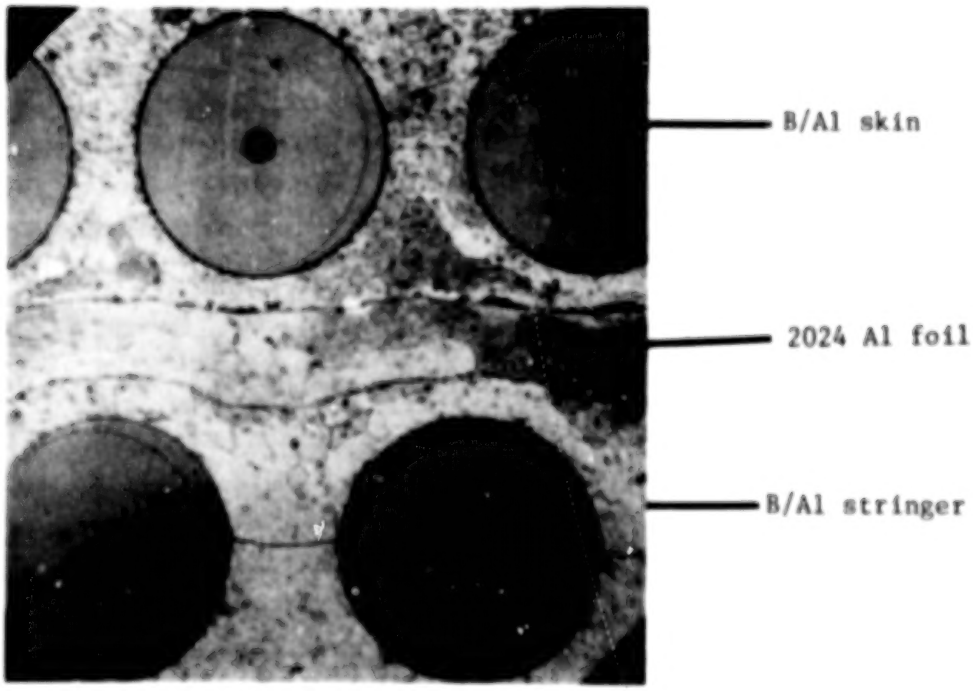

(b) B/Al skin - B/Al stringer.

L-78-32

Figure 14.- Photomicrographs of typical diffusion bonds.

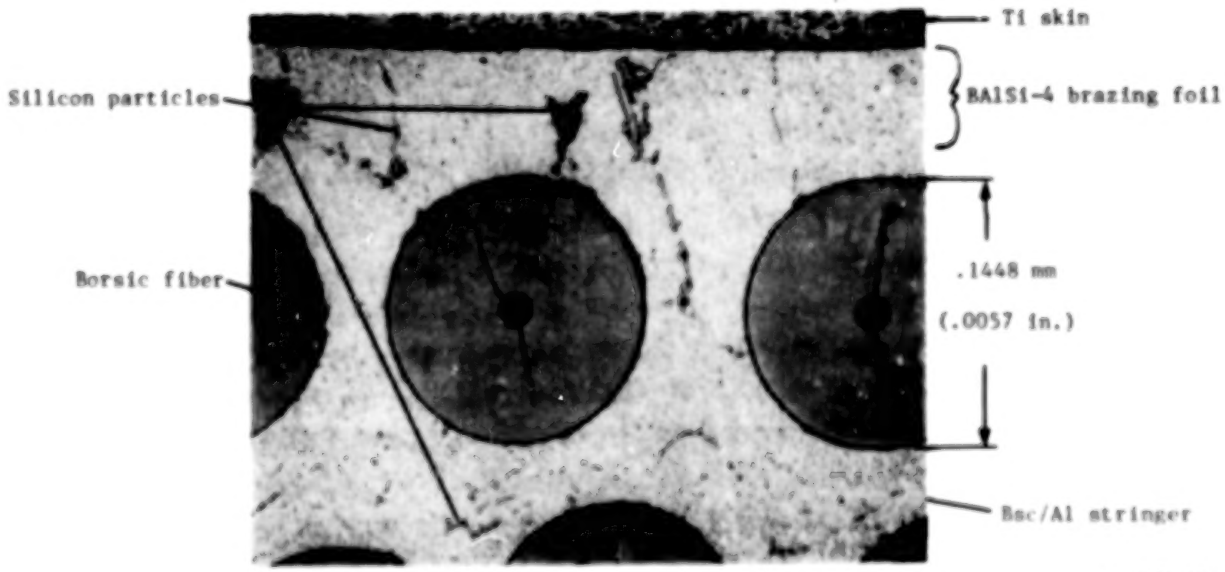

Figure 15.- Photomicrograph of typical BAlSi-4 brazed joint.

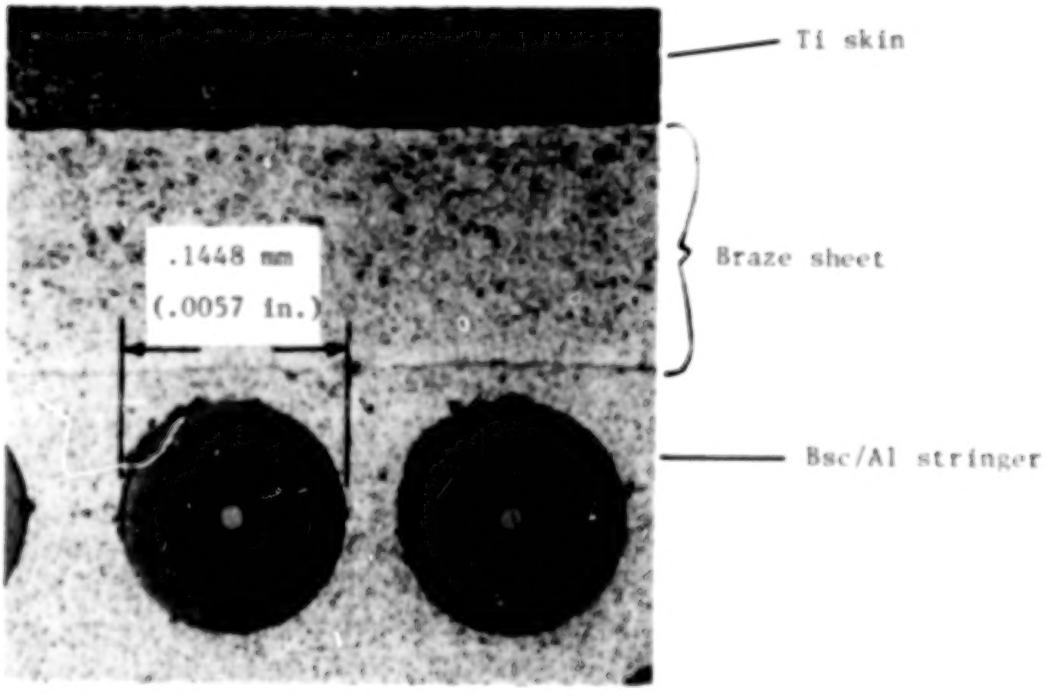

(a) Ti skin - Bsc/Al stringer.

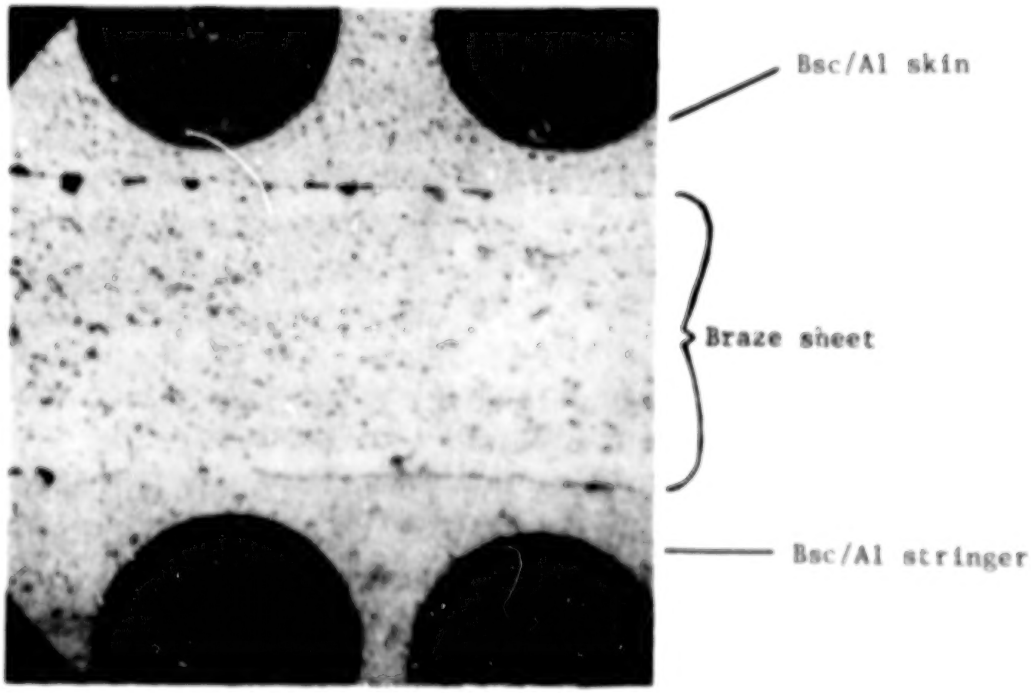

(b) Bsc/Al skin - Bsc/Al stringer.

L-78-34

Figure 16.- Photomicrographs of typical "braze sheet" joints.

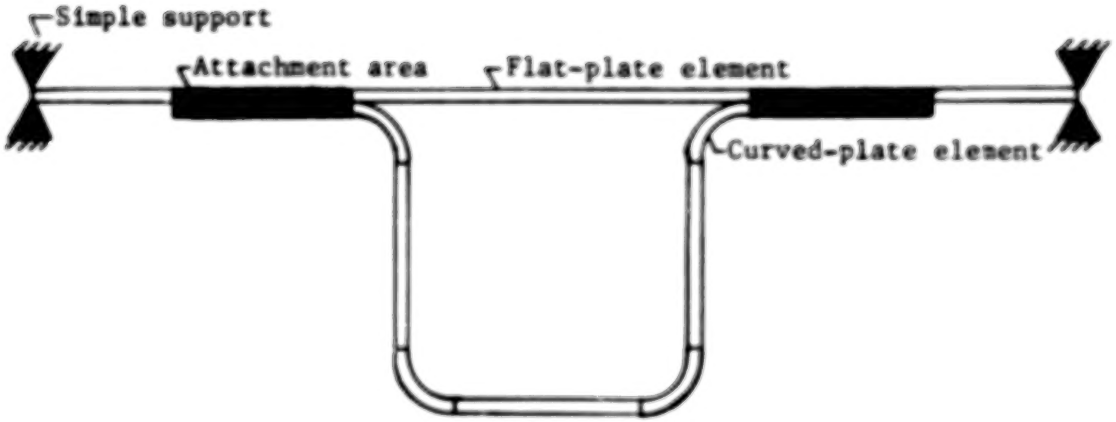

(a) Model 1 - simulates attachment by diffusion bonding, adhesive bonding, or brazing.

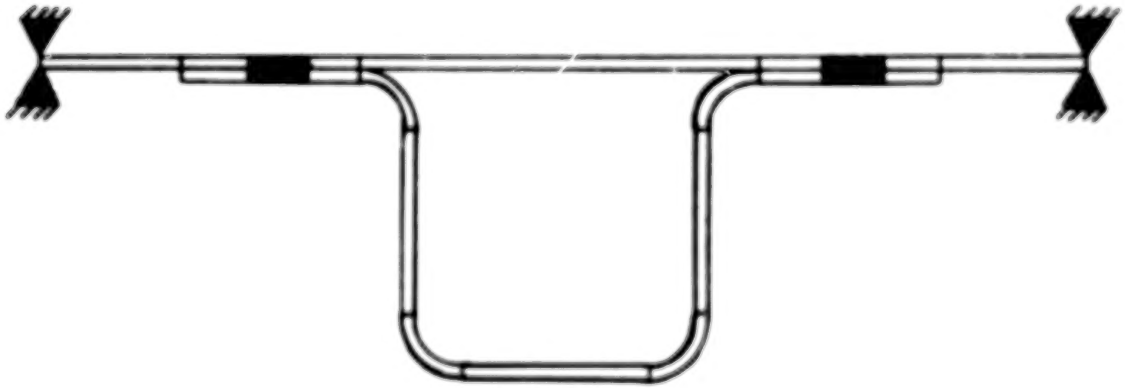

(b) Model 2 - simulates attachment by spotwelding.

Figure 17.- BUCLASP2 models used in present analyses.

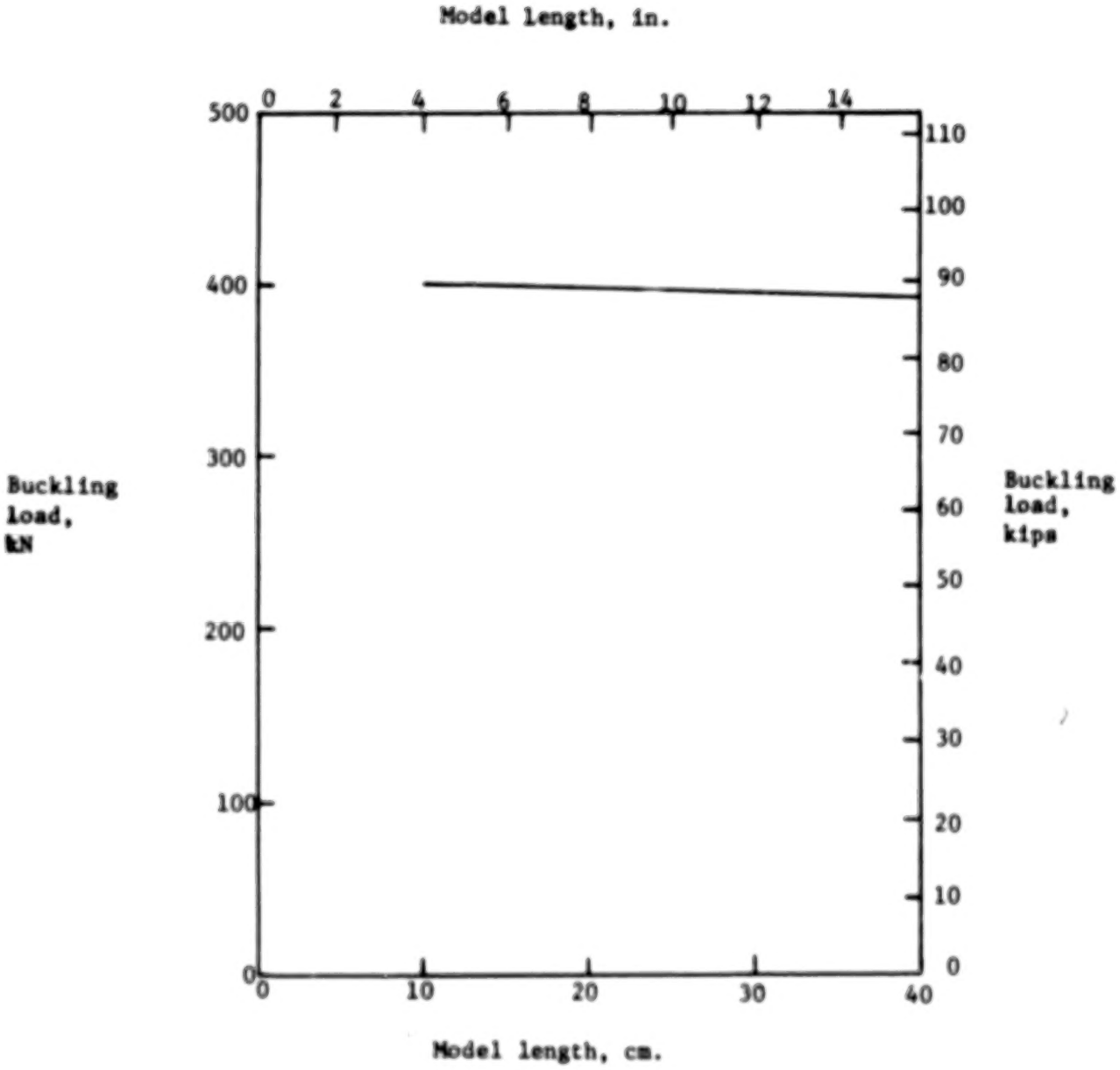

Figure 18.- Variation of analytical buckling load with model length.

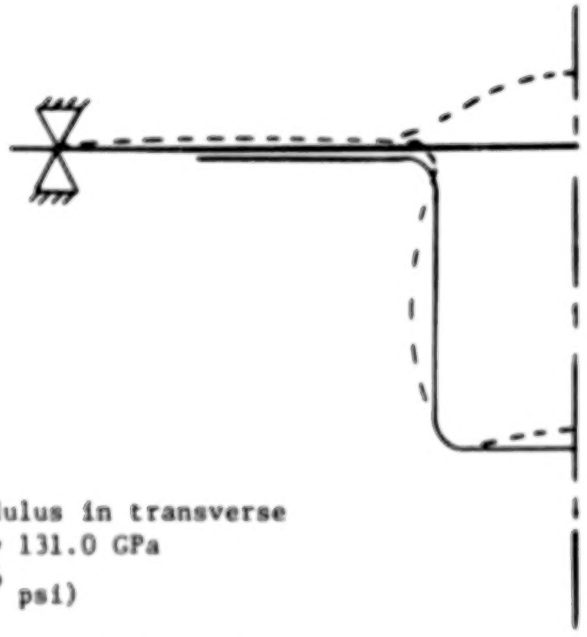

----Young's Modulus in transverse direction = 131.0 GPa (19.0×10^6 psi)

——Original skin-stringer shape

Figure 19.- Typical mode shape of panel cross section from BUCLASP2 analyses.

1. Report No.	2. Government Accession No.	3. Recipient's Catalog No.
NASA TP-1121		

4. Title and Subtitle	5. Report Date
EFFECTS OF FABRICATION AND JOINING PROCESSES ON COMPRESSIVE STRENGTH OF BORON/ALUMINUM AND BORSIC/ALUMINUM STRUCTURAL PANELS	April 1978
	6. Performing Organization Code

7. Author(s)	8. Performing Organization Report No.
Dick M. Royster, H. Ross Wiant, and Robert R. McWithey	L-11728
	10. Work Unit No. 743-01-22-01
9. Performing Organization Name and Address NASA Langley Research Center Hampton, VA 23665	11. Contract or Grant No.
	13. Type of Report and Period Covered Technical Paper
12. Sponsoring Agency Name and Address National Aeronautics and Space Administration Washington, DC 20546	14. Sponsoring Agency Code

15. Supplementary Notes
Dick M. Royster and Robert R. McWithey: Langley Research Center.
H. Ross Wiant: Vought Corporation, Hampton, Virginia.

16. Abstract

Processes for forming and joining boron/aluminum and Borsic/aluminum to themselves and to titanium alloys have been studied at the NASA Langley Research Center. Composite skin and titanium skin panels were joined to composite stringers by high strength bolts, by spotwelding, by diffusion bonding, by adhesive bonding, or by brazing. The effects of the fabrication and joining processes on panel compressive strengths are discussed. Predicted buckling loads are compared with experimental data.

17. Key Words (Suggested by Author(s))

Boron/aluminum
Borsic/aluminum
Titanium
Skin-stringer panels
Brazing
Diffusion bonding
Adhesive bonding

18. Distribution Statement

Unclassified - Unlimited

Subject Category 24

19. Security Classif. (of this report)	20. Security Classif. (of this page)	21. No. of Pages	22. Price*
Unclassified	Unclassified	52	$5.25

* For sale by the National Technical Information Service, Springfield, Virginia 22161

NASA-Langley, 1978